ON THE MAGNON BOSE EINSTEIN CONDENSATION IN FERROMAGNETIC FILM

A Dissertation

by

FUXIANG LI

Submitted to the Office of Graduate and Professional Studies of
Texas A&M University
in partial fulfillment of the requirements for the degree of

DOCTOR OF PHILOSOPHY

Chair of Committee,	Valery L. Pokrovsky
Committee Members,	Artem G. Abanov
	Wenhao Wu
	Peter Kuchment
Head of Department,	George Welch

December 2014

Major Subject: Physics

ABSTRACT

Bose-Einstein condensation (BEC) is one of the most intriguing macroscopic quantum phenomena. It has been observed in a variety of different systems, including ultracold atoms and ensembles of quasiparticles. In this work we concentrate on the magnon Bose-Einstein condensation observed in ferromagnetic yttrium iron garnet (YIG) film. In contrast to the cold atomic system, the magnon BEC proceeds at room temperature. We first review the basic theory of magnons in ferromagnetic film and discuss the recent experimental results on magnon BEC. The magnon spectrum in YIG film has two minima of energy at nonzero wavevectors Q and $-Q$. Therefore, in principle two condensates can appear. It is very important for observable condensation phenomena how the condensed magnons are distributed between the two minima and whether two condensates are coherent. Previous theoretical and experimental studies ignored both these problems. In this dissertation we address these important questions. Starting from the microscopic model describing the ferromagnetic film, we analytically calculate the interaction of condensates. It depends on thickness of the film d and external magnetic field H_0. In comparatively thick films (1-5 μm)the magnons of the same condensate attract each other, whereas the magnons of different condensate repulse. It leads to spontaneous violation of the mirror symmetry predicted by our theory. As a consequence, the numbers of condensed magnons in the two minima are not equal. This result explains the rather low contrast in the interference pattern observed in experiments by the real space Brillouin light scattering methods. We also find that the dipolar interaction that does not conserve the magnon number generates a special type of interaction that leads to the coherence between two condensates and to the existence of two types

of condensates with sum of their phase equal to either 0 or π. The existence of the interference pattern violates also the translational symmetry of the condensate. The corresponding excitations are Goldstone modes that we call "zero sound'. We calculated its spectrum. We also calculated how the condensate depends on the thickness of film and external magnetic field and discovered that , in the range of thickness $0.1 - 03$ μm the phase transition to the phase with equal condensate densities proceeds. This transition as well as transition between $0-$ and $\pi-$ phases can be driven by external magnetic field.

Next we study the relaxation rate of condensed magnons. There are two important time scales in the formation of magnon BEC, that is, the thermalization time $\tau_{\rm th}$ and the life time $\tau_{\rm l}$. In order to generate and observe BEC, the condition $\tau_{\rm th} \gg \tau_{\rm l}$ must be fulfilled. Experimentally the thermalization time is of the order of 100 ns. The relaxation is due to the magnon-magnon interaction conserving the magnon numbers. The lifetime is found to be of the order of 1 μs, and was thought to be due to the magnon-phonon interaction which doesn't conserve the magnon numbers. However the calculation of lifetime due to magnon-phonon interaction disagrees with the experimental values. Here we calculate the lifetime due to three magnon processes in a ferromagnetic film with finite thickness. Our calculation gives a lifetime of the order of 10 μs, which is almost of the same order of magnitude with the one provided by magnon-phonon interaction. This means that the three magnon processes provide an important channel for the relaxation of condensed magnons.

DEDICATION

To my beloved grandmother.

ACKNOWLEDGEMENTS

I would like to give my special and sincere thanks to my advisor, Professor Valery Pokrovsky for his direct instructions on this work and his teaching in condensed matter physics. His help, encouragements and guidance in both of my studies and life are the most valuable and precious things throughout my graduate life. His deep insights and wide knowledge in physics have benefited me a lot and will continue to benefit me in my future career.

I would like to thank Professor Saslow for his helpful discussions and suggestions in the preparation of this work. My progress in physics would be impossible without the help and collaborations with Dr. Abanov, Dr. Nattermann and Dr. Sinistyn.

I thank those who presented me wonderful lectures in the Physics department. I learned a lot from the Quantum Field Theory of Dr. Bhaskar Dutta, from the Quantum Optics of Dr. M. Suhail Zubairy, and from the Quantum Theory of Solids of Dr. Alexander Finkelstein.

Throughout the graduate life, I have always been immersed in the discussions with my friends: Wei Zhao, Chen Sun, Ning Su, Junchen Rong, Wenchao Ge and Zeyang Liao, and so on. It is because of these friends that my life become not so boring.

Finally, I thank the support of my wife.

NOMENCLATURE

BEC Bose-Einstein condensation

YIG Yttrium-iron garnet

BLS Brillioun light scattering

2D 2 dimension

3D 3 dimension

DM Dzyaloshinsky-Moriya

TABLE OF CONTENTS

Page

LIST OF FIGURES

FIGURE Page

1. INTRODUCTION

Bose-Einstein condensation (BEC), one of the most intriguing macroscopic quantum phenomena, has been observed in equilibrium systems of Bose atoms, like ^{4}He [42, 1], ^{87}Rb [4] and ^{23}Na [17]. Recent experiments have extended the concept of BEC to non-equilibrium systems consisting of photons [46] and of quasiparticles, such as excitons [10], polaritons [43, 5, 2] and magnons [87, 8, 21]. Among these, BEC of magnons in films of Yttrium Iron Garnet (YIG), discovered by the group of Demokritov [21, 27, 19, 20, 18, 26, 25, 28, 66], is distinguished from other quasiparticle BEC systems by its room temperature transition and two-dimensional anisotropic properties. In this thesis, we will theoretically study the phenomena of magnon Bose-Einstein condensation observed in YIG film [53]. The peculiarity of the spin-wave energy spectrum of the YIG film is that it has two energetically degenerate minima. Therefore it is possible that the system may have two condensates in momentum space [52]. An experiment by Nowik-Boltyk *et al.* [66] indeed shows a low-contrast spatial modulation pattern, indicating that there is interference between the two condensates. Current theories [85, 71, 70, 72, 58, 84] do not describe the appearance of coherence or the distribution of the two condensates. Our theory explains the reason of low-contrast interference pattern and agrees well with the experiment. We predict a new kind of collective oscillation, called zero sound. We also study the relaxation of condensed magnons due to three magnon processes in the ferromagnetic film with finite thickness.

1.1 Bose-Einstein condensation of cold atoms

The concept of Bose-Einstein Condensation (BEC) was first introduced by Einstein in 1925 by applying the statistical approach developed by Bose for Bosons with

conserved number of particles. It describes a macroscopic quantum phenomena in which under some conditions, a sufficiently large number of Bosonic particles collapse to a single quantum state with the lowest possible energy. The formation of a collective quantum state is purely due to the quantum statistical properties of the Bosonic particles that tend to stay together. For system with a fixed number of non-interacting particles, BEC occurs when the quantum fluctuation is of the same order of magnitude with thermal fluctuation, that is: $\frac{\hbar^2}{2ml^2} = k_B T_c$, with $\hbar$, k_B the Plank constant and Boltzman constant, respectively. Also, T_c is the transition temperature of BEC, l is the length of spacing between particles, and m is the mass of particle. By using $l = 1/n^{1/3}$ with n the density of particles, we obtain the expression for transition temperature:

$$k_B T_c = \frac{\hbar^2 n^{3/2}}{2m} \tag{1.1}$$

This simple argument gives the same result, up to a numerical factor, as that obtained by exact calculation which can be found in any textbook of Statistical Physics (for example, in [51]).

Shortly after the prediction of Einstein, the discovery of superfluidity of liquid ^{4}He [42, 1] indirectly confirms the idea of BEC. Although this system is strongly interacting and apparently differs from that considered by Einstein, the BEC is assumed to underlie the effect of superfluidity of ^{4}He [54, 7]. The pure BEC system was not realized, until 70 years later when the BEC of dilute cooled atomic gases was observed [4, 17]. The reason why the experimental discovery happened so late can be partly explained by Eq. 1.1. The particle density n must not be two high otherwise either the interacting effect becomes important or the atoms form molecules. As a result, the transition temperature is rather low, of the order of 10^{-6} K. Such a

temperature was reached only after the great improvement of cooling techniques in experiment [59, 55, 52].

1.2 Bose-Einstein condensation of quasiparticles

Besides real atomic gases, it was also predicted that gases of different types of quasiparticles, like excitons in semiconductors, would be good candidates for BEC. Dated back to the 1960s, there were already several theoretical discussions of the possibility of condensation in systems of longitudinal electric modes [29] and excitons [6]. Compared to real atoms, the BEC of quasiparticles have two advantages: First, the effective mass of quasiparticles are usually much smaller than that of real atoms. This makes the transition temperature relatively larger because it is inversely proportional to the mass. Second, the density of quasiparticle system can be easily increased by increasing the external pumping without worrying about the formation of molecules. However, quasiparticle has a finite lifetime due to the inevitable interactions between themselves or with phonons in the solids. This finite lifetime requires that the BEC must be realized in a time scale much smaller than it. This means that BEC of quasiparticles happens in a non-equilibrium state, or strictly speaking, quasi-equilibrium. This is not a big problem, because it just brings the BEC into another time scale while the effect is not cancelled. Actually, any BEC, including BEC of atoms, is always in quasi-equlibrium. To date, BEC of quasiparticles has been reported in systems of excitons [63, 10], polaritons [43, 5, 3], photons in optical microcavity [46] and magnons in ^3He[8] and Yttrium-Iron-Gargnet film[21]. Note that in a quite different context, magnon BEC in antiferromagnetic material $TlCuCl_3$ has also been discussed [64, 30, 90]

1.3 Magnon Bose-Einstein condensation in YIG film

The theoretical prediction of magnon BEC in ferromagnetic materials can be dated back to 1980s [36, 37, 38, 35], . However, no fundamental constrains were suggested in all works, which would prevent the observation of BEC of magnons. It was also proposed that the magnon BEC could be one of the explanations of microwave radiation from the bottom of spin wave spectrum in YIG samples [61]. However, no sufficient experimental data were provided to prove this suggestion in early days.

YIG material is very suitable for the realization of magnon BEC. The effective mass of magnons near the minimum point (or points) is the order of electron mass, which is at least 3 orders smaller than that of atoms. Moreover, in YIG, magnons can be easily excited by parametric pumping with small loss. At the same time, the lifetime of magnons near the minimum points is very long due to weak coupling with phonon system, compared to the thermalization time due to sufficiently strong magnon-magnon interaction conserving magnon numbers.

1.4 Outline of the work

Section 2 presents a basic introduction to spin wave theory. Both classical and quantum theory are described after the introduction of all kinds of magnetic introductions including exchange interactions, dipolar-dipolar interactions, anisotropy and so on. Then we introduce the experimental discovery of magnon Bose-Einstein condensation in Yttrium Iron Garnet by discussing the experimental setup and its detection method, Brillouin light scattering. How the spontaneous appearance of coherence of magnon BEC was confirmed in the experiment and the kinetics of magnons in phase space are mainly stressed.

In Section 3, we give a detailed account of our work on magnon BEC. By taking

into account the fourth order interaction of magnons, we analytically show that the numbers of condensed magnons in the two condensates are not equal to each other. This is a spontaneous breaking of a mirror symmetry induced by the magnon interactions even though the mirror symmetry of the system is reserved. Our theory points out that by changing thickness of YIG film or external magnetic field, it is possible to vary the ratio of numbers of magnons in condensates. There are two different phases with equal or not equal numbers of magnons in the two condensates. We call these two cases as symmetric phase and asymmetric phase, and a phase diagram is given. We also predict a new collective mode of excitation, called zero sound.

In Section 4, we present the calculation of the relaxation of condensed magnons due to three magnon processes when the film has finite thickness. It is found to be of the same order of magnitude with that due to magnon-phonon interaction. This study is important not only in the understanding of magnon BEC, but also in the understanding of inverse spin Seebeck effect recently discovered in the YIG/Pt heterostructure.

Section 5 is the conclusion.

2. SPIN WAVE PHYSICS IN FERROMAGNETIC FILM

Spin wave is a kind of collective motion of spins in magnetic materials, not restricted to ferromagnetic materials. From the point view of quantum mechanics, spin wave can be treated in a convenient way by introducing the concept of an elementary excitation: magnon. Physically, the spin wave forms when the spins are made to tilt from their equilibrium configuration, and due to the increase of local magnetic interaction energy, local disturbance propagates through the magnetic media in order to restore to the original equilibrium configuration, as shown is Fig. 2.1. Spin waves carry energy and momentum. In ferromagnets they also carry spin or magnetization. Therefore, they determine the dynamics and thermodynamics of magnets. The measurement of spin wave dispersion are traditionally used to determine fundamental parameters, such as exchange constant, anisotropy constant, dissipation and so on. Spin wave quanta, or magnon, carries spin angular moment with magnitude 1. Therefore, it is considered to be a promising carrier of spin current. Thanks to the rapid development of nanomagnetism and spintronics, a new field, magnonics, emerges towards future application based on the utilizing and manipulation of spin waves [89, 23].

In this section, we mainly introduce the basic classical and quantum theory of spin waves, especially in ferromagnetic film. We also discuss the important experimental discovery of Bose-Einstein condensation of magnon in Yttrium Iron Garnet film.

2.1 Different magnetic interactions

Before we start to investigate the energy spectrum and spin wave properties, let's review the different interactions in magnetic materials, including exchange interaction, anisotropy, dipolar-dipolar interaction and Dzyaloshinsky-Moria interaction

and so on.

2.1.1 Exchange interaction

The most important interaction in ferromagnetic substances is the exchange interaction of atoms. This interaction is responsible for the spontaneous magnetization of ferromagnets. The exchange interaction results from the electrostatic interaction, i.e. the Coulomb interaction of electrons and the symmetry of the wave function of the system related with the Pauli principle. It is usually described as Heisenberg model, defined in terms of spin operators $\mathbf{S}_i$ on a lattice model:

$$H_{ex} = \sum_{ij} J_{ij} \mathbf{S}_i \cdot \mathbf{S}_j \tag{2.1}$$

in which J_{ij} describes the exchange integral of spins between lattice i and j. A characteristic property of this interaction is that it is independent of the orientation of the magnetization relative to the lattice and does not depend on the direction of the total spin. According to Goldstone theorem, a system of this kind of interaction possesses a kind of Goldstone mode which is gapless. In this case, it is just the spin wave. However, this mode will become gapped if we include other weaker, relativistic interactions, such as dipolar interaction which breaks the continuous symmetry of exchange interaction.

For Eq. 2.1, if $J < 0$, we call the exchange interaction being "ferromagnetic", i.e. such that the parallel position of the moments, or spins, is energetically favourable. Other more complex cases may appear. For ferrimagnets, the structures can be formed of two oppositely magnetized sub-lattices whose magnetizations are different and which therefore are not completely compensated. For the case of complete compensation, it corresponds to antiferromagnets.

Helical magnetic structures may appear if we have special conditions for J_{ij}.

Consider only the nearest neighbor integral J_1 and next nearest neighbor integral J_2 are important, and we have: $J_1 < 0$ and $J_2 > 0$, and $|J_1| > |J_2|$. Then one can expect that due to negative J_1, the ground state intends to align all the spins, however, the positive J_2 will make a small deviation of neighboring spins.

Schematics of ferromagnet, ferrimagnet, antiferromagnet and helical magnet are shown in Fig. 2.2

On the macroscopic level, the energy is expressed in terms of a macroscopic parameter, the magnetization moment $\mathbf{M}$, which is a continuous function of coordinates. That is to say, in the limit that the spin wavelength is large compared with the lattice constant a, i.e. the wave number $k \ll 1/a$, the spin wave may be treated macroscopically.

The exchange interaction in Eq. 2.1 can be rewritten in terms of $\mathbf{M}$. The result is a combination of a constant plus a non-uniform term, as shown in the following:

$$U_{\text{ex}} = \frac{1}{2}\alpha_{ik}\frac{\partial \mathbf{M}}{\partial x_i}\frac{\partial \mathbf{M}}{\partial x_k} \tag{2.2}$$

The expression is constructed so that it is independent of the absolute direction of $\mathbf{M}$. In uniaxial crystals, the symmetric tensor α_{ik} of rank two has components $\alpha_{xx} = \alpha_{yy} \equiv \alpha_1$, $\alpha_{zz} \equiv \alpha_2$ where the z=axis is the axis of symmetry of the crystal; in cubic crystals, $\alpha_{ik} = \alpha\delta_{ik}$. Specifically:

$$U_{\text{ex}} = \frac{1}{2}\alpha\left[(\partial_x \mathbf{M})^2 + (\partial_y \mathbf{M})^2 + (\partial_z \mathbf{M})^2\right] \tag{2.3}$$

2.1.2 Anisotropy energy

Anisotropy of ferromagnets is due to the relativistic interaction between their atoms, and these interactions are comparatively weak.

The calculation of the anisotropy energy from the microscopic theory would require the use of quantum perturbation theory, the energy of the perturbation being represented by the terms in the Hamiltonian of the crystal which pertain to the relativistic interactions. The general form of the desired expressions, however, can be deduced without such calculations, only from simple arguments concerning symmetry. The relativistic interactions contains two terms in powers in electron spin vector operators: the spin-orbit and spin-spin interactions, respectively. Both are very small because they are proportional to v^2/c^2, where v is of the order of magnitude of the velocities of atomic electrons, and c is the velocity of light. The anisotropy energy U_{anis} should be invariant under time reversal. Because the magnetization $\mathbf{M}$ changes sign under time reversal, therefore the anisotropy energy must be an even function of the components of $\mathbf{m}$, the unit vector of $\mathbf{M}$.

For uniaxial and biaxial crystals, the expansion of anisotropy energy begins with squares of these components, and may be written:

$$U_{\text{aniso}} = K_{ik} m_i m_k \tag{2.4}$$

where K_{ik} is a symmetrical tensor of rank two, whose components, like U_{aniso} itself, have the dimensions of energy density.

For ferromagnetic crystals of the cubic system, the properties differ considerably from those of uniaxial crystals. This is because the only quadratic combination which is invariant under the cubic symmetry transformations and which can be formed from the components of the vector $\mathbf{m}$ is $\mathbf{m^2 = 1}$. The first nonvanishing term in the expansion of the anisotropy energy for a cubic crystal is therefore of the fourth, not the second, order. For this reason, the magnetic anisotropy effects in cubic crystals are in general weaker than in uniaxial and biaxial crystals. Cubic symmetry allows

only one independent fourth-order invariant which depends on the direction of **m**. The anisotropy energy of a cubic ferromagnet can therefore be expressed as :

$$U_{\text{aniso}} = -\frac{1}{2}K(m_x^4 + m_y^4 + m_z^4) \tag{2.5}$$

In the formation of domain walls, anisotropy is very important in determining the width of domain wall structures.

On the microscopic level, the anisotropy can be introduced by generalizing the above mentioned Heisenberg model in which the SU(2) symmetry is conserved. In real crystals, the elementary cell and the environment of the magnetic ions have no rotational symmetry, the Heisenberg Hamiltonian has to be generalized as:

$$H = \sum_{\alpha,\beta} \sum_{ij} J_{ij}^{\alpha\beta} S_i^\alpha S_j^\beta \tag{2.6}$$

where S_i^α is the α component of spin operator on lattice i, and $J_{ij}^{\alpha\beta}$ is a tensor.

Not all the components of $J_{ij}^{\alpha\beta}$ are nonzero due to the specific symmetry of the lattice structure. For example, in the case of uniaxial structure, in which only one direction is favored or disfavored, we have:

$$H_{\text{aniso}} = J \sum_{ij} \left[S_i^x S_j^x + S_i^y S_j^y + (1+\lambda) S_i^z S_j^z \right] \tag{2.7}$$

where we assume thhat the z-axis is the uniaxial axis, λ describes the anisotropy. If $\lambda > 0$ ($\lambda < 0$) then z-axis is energetically unfavorable (favorable).

2.1.2.1 Dzyaloshinsky-Moriya interaction

A special anisotropy, which emerges due to inversion symmetry breaking of the lattice, is the Dzyaloshinsky-Moriya (DM) anisotropy. It leads to the following ad-

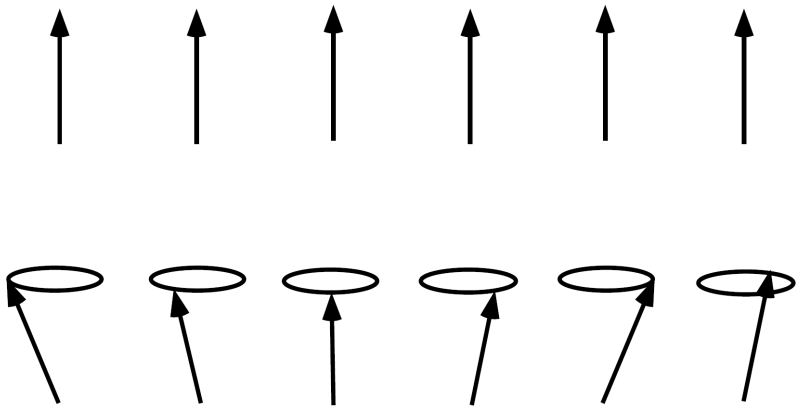

Figure 2.1: Schematic of spin wave. Spins, or magnetic moment $\mathbf{M}$, rotate around static external magnetic field $\mathbf{H}$.

ditional term in the Hamiltonian [24, 62],

$$H_{\mathrm{DM}} = \sum_{ij} \mathbf{D}_{ij} \cdot (\mathbf{S}_i \times \mathbf{S}_j) \tag{2.8}$$

Since the components of the anisotropy vector $\mathbf{D}_{ij}$ are related to the value of the corresponding exchange couplings, one usually considers the anisotropy along the bonds with the largest exchange coupling.

On the macroscopic level, the Dzyaloshinsky-Moriya interaction can be expressed in terms of $\mathbf{M}$:

$$U_{\mathrm{DM}} = \gamma \mathbf{M} \cdot \nabla \times \mathbf{M} \tag{2.9}$$

This interaction will makes the uniform ferromagnetic solution unstable. As can be seen by combing Eq. 2.9 and Eq. 2.3, even $\alpha > 0$ doesn't guarantee that the uniform state is stable. In stead a helical structure becomes stable. Let's write:

$$\mathbf{M}(\mathbf{r}) = M(\mathbf{m}_1 \cos \mathbf{k} \cdot \mathbf{r} - \mathbf{m}_2 \sin \mathbf{k} \cdot \mathbf{r}) \tag{2.10}$$

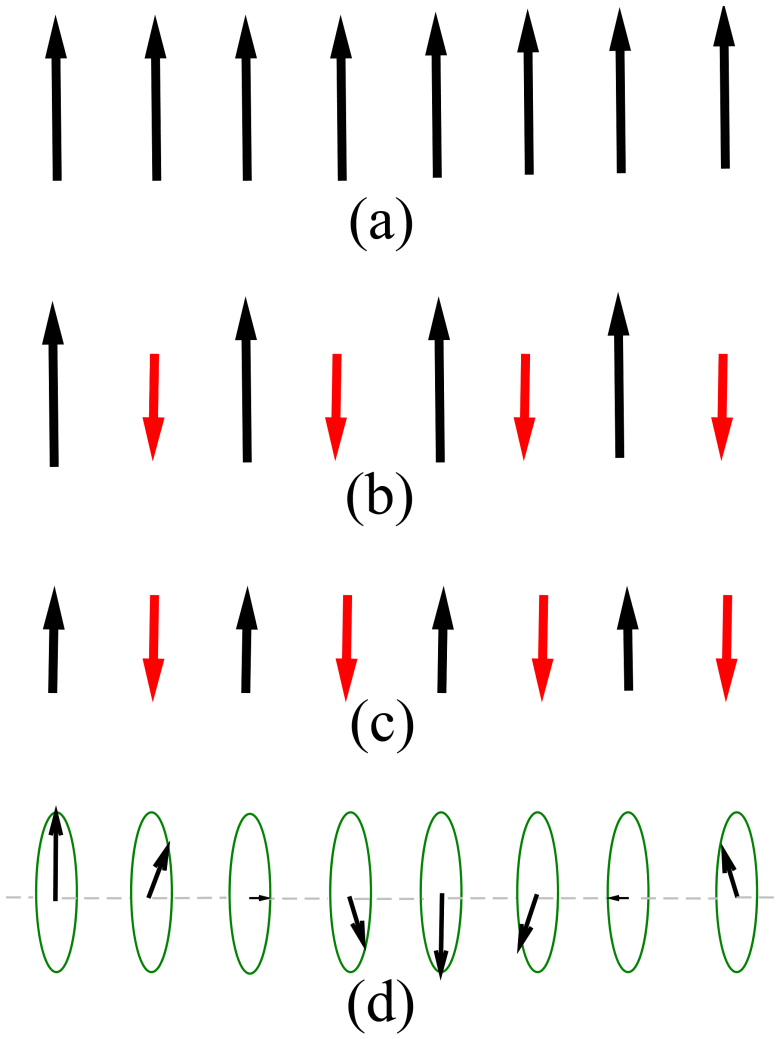

Figure 2.2: Schematics of ferromagnet, ferrimagnet, antiferromagnet and helical magnet.

where $\mathbf{m}_1$ and $\mathbf{m}_2$ are two mutually perpendicular real unit vectors. Substitution of the above solution into the energy expression combined from Eq. 2.9 and Eq. 2.3, we have:

$$U = M^2\gamma\mathbf{k}\cdot\mathbf{m}_1\times\mathbf{m}_2 + \frac{1}{2}\alpha M^2k^2 \tag{2.11}$$

This experssion has a minimum as a function of $\mathbf{k}$ if the vectors $\mathbf{k}$ and $\mathbf{m}_1\times\mathbf{m}_2$ are colinear(parallel if $\gamma < 0$ and antiparallel if $\gamma > 0$. Furthermore:

$$k = \gamma/\alpha \tag{2.12}$$

Actually the DM interaction is proportional to v^2/c^2, which renders it much smaller than the exchange interaction. This means that $\gamma \ll \alpha/a$, where a is the lattice constant. Therefore, $k \ll 1/a$. Thus the presence of DM interaction term causes the occurence of a helcial magnetic structure. The magnetic moments of the atoms lie in planes perpendicular to the direction of $\mathbf{k}$ and the directions of the moments rotate slowly in successive layers of atoms. The pitch of helix is $2\pi/k$ which is much large than a, is the period of the superlattice. The helix is in general incommensurate with the crystallographic periods.

2.1.3 Dipolar interaction

As mentioned above, the dipole-dipole interactions are rather weak and typically do not dominate the behavior of magnetic ordering and related physical observables . As in the classical energy between magnetic moments, the dipolar-dipolar interaction can be written as

$$H_D = \frac{1}{2}\sum_{ij,i\neq j}\mu^2\frac{3(\mathbf{S}_i\cdot\hat{\mathbf{R}}_{ij})(\mathbf{S}_j\cdot\hat{\mathbf{R}}_{ij}) - \mathbf{S}_i\cdot\mathbf{S}_j}{R_{ij}^3} \tag{2.13}$$

where the sums are over the sites $\mathbf{R}_i$ of the lattice and $\hat{\mathbf{R}_{ij}}$ are unit vectors in the direction of $\hat{\mathbf{R}}_{ij} = \mathbf{R}_{ij}/|R_{ij}| = \mathbf{R}_i - \mathbf{R}_j$. Here, $\mu = g\mu_B$ is the magnetic moment associated with the spins, where g is the effective g-factor and $\mu_B = \frac{e^2}{2mc}$ is the Bohr magneton.

This contribution to the energy becomes important if the isotropic exchange Hamiltonian does not allow ordering at finite temperature. A famous example is the two-dimensional Heisenberg magnets, in which the Mermin-Wagner theorem guarantees that in the presence of $SU(2)$ symmetry there is no magnetic long-range order at any finite temperature. The dipole-dipole interaction term, instead, has a lower symmetry and therefore suppresses the fluctuation and supports the existence of two-dimensional magnet. Also, the dipolar interaction opens the possibility of a nonzero gap in the excitation spectrum, because in that case the Goldstone theorem does not apply. Because dipolar interaction describes interactions between spins at long distances, i.e., dipolar interaction is a long-range interactions, it will mainly modify the spectrum structure at low wave vectors $k \to 0$.

2.2 Classical theory of spin wave: Landau-Lifthiz equation

The classical theory is valid when the spin wavelength is large compared with the lattice constant a . In this case, spin wave spectrum, or the magnon specturm $\omega(\mathbf{k})$ depends only on macroscopic parameters of the magnetic materials. It is exactly analogous to the definition of the long-wave phonon spectrum in terms of macroscopic parameters (elastic moduli).

The motion of magnetic moment is described by Landau-Liftshiz equation [16, 39, 40, 41, 78, 79]:

$$\frac{\partial \mathbf{M}}{\partial t} = \frac{g|e|}{2mc}\mathbf{H}_{\text{eff}} \times \mathbf{M} \tag{2.14}$$

where $e = -|e|$ and m are the electron charge and mass, and g the gyromagnetic ratio of the ferromagnet. $\mathbf{H}_{\text{eff}}$ is the effective magnetic field, which can be given by the variation of free energy with respect to $\mathbf{M}$:

$$\mathbf{H}_{\text{eff}} = -\frac{\delta F}{\delta \mathbf{M}} \tag{2.15}$$

Including only the exchange interaction and Zeeman interaction

$$F = \int dV \left[f_0(M) + U_{\text{non-u}} - \mathbf{M} \cdot \mathbf{H} - H^2/8\pi \right] \tag{2.16}$$

Here $f_0(M)$ is the free energy density of a uniformly magnetized body at $\mathbf{H} = 0$. It takes account only of exchange interaction and is independent of the direction of $\mathbf{M}$; $U_{\text{non-u}}$ is the additional part of exchange interaction due to the slow change of direction of $\mathbf{M}$ with rescpet to the uniformly magnetized body, which is already given by Eq. 2.2.

Varying the integral in Eq. 2.16, we can get the expression for effective field:

$$\mathbf{H}_{\text{eff}} = -\alpha_{ik} \frac{\partial^2 \mathbf{M}}{\partial x_i \partial x_k} + \mathbf{H} \tag{2.17}$$

from which we have neglected a term proportional to $\mathbf{M}$ derived from the $f_0(M)$ term, because it will disappear once substituted into the equation of motion of $\mathbf{M}$, Eq. 2.14

Let's consider the spin wave solution to Eq. 2.14. We assume only one-domain sample with uniform magnetization $\mathbf{M}_0$ in z direction. We consider only spin wave with wavelength much longer than the lattice constant, but much smaller than the size of the sample. That is, we can think of the sample to be infinite. The spin wave

is a small deviation from $\mathbf{M}_0$. If we write

$$\mathbf{M} = \mathbf{M}_0 + \mathbf{m} \tag{2.18}$$

we need to add the constraint to $\mathbf{m}$ that $\mathbf{m} \perp \mathbf{M}_0$.

Substituting $\mathbf{M}$ into the equation of motion, Eq. 2.14 and linearize the equation by omitting the terms of the second order in $\mathbf{m}$, we have:

$$\dot{\mathbf{m}} = \gamma \alpha_{ik} \frac{\partial^2 \mathbf{m}^2}{\partial x_i \partial x_k} \times \mathbf{M}_0 \tag{2.19}$$

here $\gamma = \frac{g|e|}{mc}$.

We look for a wavelike solution of $\mathbf{m}$ with wave vector $\mathbf{k}$ and frequency ω, $e^{i(\mathbf{k}\cdot\mathbf{r}-\omega t)}$, we find:

$$i\omega \mathbf{m} = \gamma \alpha k^2 \mathbf{m} \times \mathbf{M}_0 \tag{2.20}$$

where $\alpha = \alpha_{ik} n_i n_k$. Writing explicitly the x and y components of $\mathbf{m}$ (z component is zero), we have:

$$i\omega m_x = \gamma \alpha M k^2 m_y$$
$$i\omega m_y = -\gamma \alpha M k^2 m_x$$

we can get the dispersion relation for the spin wave:

$$\omega = \gamma \alpha k^2 \tag{2.21}$$

As expected, it is symmetric with respect to $\mathbf{k}$. And in the case with only exchange

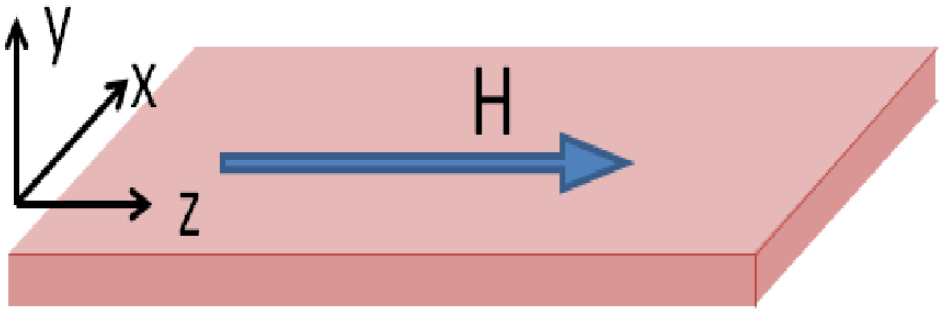

Figure 2.3: Geometry of the ferromagnetic film. The film has a thickness of d, and is supposed to be infinitely large in the plane. External magnetic field is applied in the plane, in the same direction as the magnetization $\mathbf{M}$.

interaction considered, the frequency $\omega \to 0$ as $k \to 0$, that is, it is a gapless Goldstone mode.

The effect of anisotropy and Zeeman interaction can be easily taken into account by adding the corresponding terms into the free energy. Their effects will be reflected through the effective magnetic field.

2.3 Quantum theory of magnons in ferromagnetic film

As in any macroscopic system, weakly excited states of ferromagnet may be regarded as an assembly of elementary excitations, a quasi-particle gas. The elementary excitations in an ordered distribution of atomic magnetic moments are called magnons [14, 49, 88]. Since we are dealing with quasi-particles in a crystal lattice with translational symmetry, the magnons have definite quasi-momenta, not actual momenta. The magnons obey Bose statistics, and large occupation numbers of the magnon states correspond to the classical limiting case of spin waves.

In this section, we will consider the quantum theory of magnons in a ferromagnetic film, whose geometry is shown in Fig. 2.3.

2.3.1 Holstein-Primakoff transformation

If we are interested in the lowest excitation band of magnons, then we can simulate the system by the following spin Hamiltonian containing three terms: the Zeeman interaction, exchange interaction and the dipolar interaction:

$$H = H_Z + H_{ex} + H_D \tag{2.22}$$

$$H_Z = -g\mu_B H_0 \sum_i S_i^z \tag{2.23}$$

$$H_{ex} = -J \sum_{\langle ij \rangle} \mathbf{S}_i \cdot \mathbf{S}_j \tag{2.24}$$

The in-plane external magnetic field H_0 is along z direction. We assume y axis is normal to the plane. For the exchange interaction, we consider only the nearest neighbor interaction.

Let's make the Fourier transformation for $\mathbf{S}_i$:

$$\mathbf{S}_i = \frac{1}{\sqrt{N}} \sum_{\mathbf{k}} e^{i\mathbf{k}\cdot\mathbf{r}_i} \mathbf{S}(\mathbf{k}); \tag{2.25}$$

and inversely,

$$\mathbf{S}(\mathbf{k}) = \frac{1}{\sqrt{N}} \sum_i e^{-i\mathbf{k}\cdot\mathbf{r}_i} \mathbf{S}_i \tag{2.26}$$

where N is the number of elementary cells in the film.

The Zeeman and exchange terms can be rewritten as:

$$H_{ex} + H_Z = -J \sum_{\langle ij \rangle} (\frac{1}{2} S_i^+ S_j^- + \frac{1}{2} S_i^- S_j^+ + S_i^z S_j^z) - g\mu_B H_0 \sum_i S_i^z \tag{2.27}$$

where we have introduced :

$$S^{\pm} = S^x \pm iS^y. \tag{2.28}$$

Then we have:

$$\begin{aligned} H_{ex} + H_Z &= -\frac{J}{2}\sum_{\mathbf{k}}\sum_{\boldsymbol{\delta}} e^{i\mathbf{k}\cdot\boldsymbol{\delta}}\Big[S^+(\mathbf{k})S^-(-\mathbf{k}) + S^-(\mathbf{k})S^+(-\mathbf{k}) \\ &\quad + S^z(\mathbf{k})S^z(-\mathbf{k})\Big] - g\mu_B H_0\sqrt{N}S^z(\mathbf{k}=0) \end{aligned} \tag{2.29}$$

in which $\boldsymbol{\delta}$ is the vector between two nearest neighbor lattice sites.

Notice that, up to now, $\mathbf{k}$ is defined in 3D, that is, $\mathbf{k} = (k_x, k_y, k_z)$. Due to the finite thickness, k_y is quantized, for some boundary condition, eg., $k_y = \frac{\pi n}{d}$, with n integer. In the following, when we treat the dipolar interaction, we make an approximation that only the lowest band is considered. Therefore, in the following discussion,we set $k_y = 0$. It means that $\mathbf{k}$ is always in 2 dimension, $\mathbf{k} = (k_x, 0, k_z)$.

The following procedures are to transform the non-commuting spin operators into Bosonic creation and annihilation operators. This transformation is accomplished through the Holstein-Primakoff transformation (See, e.g. [57, 65]). This method has found numerous applications and has been extended in many different directions. There is a close link to other methods of boson mapping of operator algebras; in particular to the Dyson-Maleev technique, and to a less extent to the Schwinger mapping.

The basic idea of Holstein-Primakoff transformation can be illustrated as follows. Consider a quantum spin described by operators $\hat{S}_{x,y,z}$. We can specify its state by

a ket $|S, m\rangle$ the eigenstate of $\hat{S}^2$ and $\hat{S}_z$:

$$\hat{S}^2|S, m\rangle = S(S+1)|S, m\rangle \tag{2.30}$$

$$\hat{S}_z|S, m\rangle = m|S, m\rangle \tag{2.31}$$

Now take the state with maximal projection $|S, m = +S\rangle$, the extremal weight state as a vacuum for a set of boson operators, and each subsequent state with lower projection quantum number as a boson excitation of the previous one,

$$|S, S-n\rangle \to \frac{1}{\sqrt{n!}}|(a^\dagger)^n|0\rangle \tag{2.32}$$

Each added boson then corresponds to a decrease of $\hbar$ in the spin projection. The spin raising and lowering operators $\hat{S}_\pm$ therefore correspond (in some sense) to the bosonic annihilation and creation operators, respectively.

The Holstein-Primakoff transformation can be written as:

$$S_j^+ = \sqrt{2S}\left(1 - \frac{a_j^\dagger a_j}{2S}\right)^{1/2} a_j \tag{2.33}$$

$$S_j^- = \sqrt{2S} a_j^\dagger \left(1 - \frac{a_j^\dagger a_j}{2S}\right)^{1/2} \tag{2.34}$$

$$S_j^z = S - a_j^\dagger a_j \tag{2.35}$$

In the real material we are interested in, Yttrium Iron Garnet, we can approximately assume that the effective spin $S = 14.5$, which is proved to give quite good result for the calculation of magnon spectrum. Since $S \gg 1$, we can expand the above expressions for spin operators in orders of $1/S$.

$$S_j^+ = \sqrt{2S}\left(a_j - a_j^\dagger a_j a_j/4S\right) \tag{2.36}$$

$$S_j^- \quad = \sqrt{2S}\left(a_j^\dagger - a_j^\dagger a_j^\dagger a_j/4S\right) \tag{2.37}$$

The Fourier transformation of the above expressions are is

$$S^+(\mathbf{k}) \quad = \sqrt{2S}(a_k - \frac{1}{4SN}\sum_{q,q'} a^\dagger_{q+q'-k} a_q q_{q'}) \tag{2.38}$$

$$S^-(-\mathbf{k}) \quad = \sqrt{2S}(a_k^\dagger - \frac{1}{4SN}\sum_{q,q'} a^\dagger_q a^\dagger_{q'} a_{q+q'-k}) \tag{2.39}$$

$$S^z(\mathbf{k}) \quad = \sqrt{N}S\delta_{k,0} - \frac{1}{\sqrt{N}}\sum_q a_q^\dagger a_{q+k} \tag{2.40}$$

Substitute these into the expression of $H_z + H_{ex}$ and keep only up to second orders of a_k and $a_k^\dagger$. We have, with a constant term neglected,

$$H_z + H_{ex} = \hbar \sum_{\mathbf{k}} \left(\gamma H_0 + Dk^2\right) a_k^\dagger a_k \tag{2.41}$$

in which, $D = 2JSa^2$, with a the lattice constant and $\gamma = \frac{g\mu_B}{\hbar}$

2.3.2 Treatment of dipolar interaction

As mentioned before, we are only interested in the lowest excitation band of the magnon spectrum, therefore the transverse mode corresponding to $k_y \neq 0$ is neglected. Correspondingly, the contribution of the dipolar energy to the Hamiltonian can be approximated by the uniform transverse mode. Following Refs. [71], we neglect the variation of the magnetization in the direction transverse to the film and substitute the local magnetization by its average over the transverse coordinate y. Under this approximation, the variation of magnetization $\mathbf{m}$ with respect to the original uniform magnetization $\mathbf{M}_0$ can be written as:

$$\mathbf{m}(x,z) = \int \frac{dy}{d}\mathbf{m}(x,y,z) \tag{2.42}$$

Equation of its dynamics should be considered together with Maxwell equations:

$$\nabla \times \mathbf{h}^{\mathrm{dip}} = 0 \tag{2.43}$$

$$\nabla \cdot \mathbf{h}^{\mathrm{dip}} + 4\pi \nabla \cdot \mathbf{m} = 0 \tag{2.44}$$

For the first equation, one can introduce magnetic potential ψ, satisfying

$$\mathbf{h}^{\mathrm{dip}} = -\nabla \psi \tag{2.45}$$

Correspondingly, the second equation becomes:

$$\nabla^2 \psi = 4\pi \nabla \cdot \mathbf{m} \tag{2.46}$$

Together with the boundary condition on the surface at $x = \pm d/2$ ($\mathbf{m} = 0$ outside of the film), we can solve this 1-Dimensional static magnetic problem. First we make a Fourier transformation of ψ and $\mathbf{m}$ in the x and z direction:

$$\psi(x, y, z) = \frac{1}{\sqrt{V}} \sum_{\mathbf{k}} e^{i\mathbf{k}\cdot\mathbf{r}} \psi_k(y) \tag{2.47}$$

$$\psi_k(y) = \frac{d}{\sqrt{V}} \int dx dz e^{-i\mathbf{k}\cdot\mathbf{r}} \psi(x, y, z) \tag{2.48}$$

and

$$\mathbf{m}(x, z) = \frac{1}{\sqrt{V}} \sum_{\mathbf{k}} e^{i\mathbf{k}\cdot\mathbf{r}} \mathbf{m}(k) \tag{2.49}$$

$$\mathbf{m}(\mathbf{k}) = \frac{d}{\sqrt{V}} \int dx dz e^{-i\mathbf{k}\cdot\mathbf{r}} \mathbf{m}(x, z) \tag{2.50}$$

In the above equations, both $\mathbf{k}$ and $\mathbf{r}$ should be understood as two dimensional

vectors.

Then Eq. 2.46 becomes:

$$\left(\frac{d^2}{dy^2} - k^2\right)\psi_k(y) = 4\pi i\left(k_x m_x(k) + k_z m_z)\right) + 4\pi\partial_y m_y(k) \tag{2.51}$$

in which the last term vanishes anywhere except on the surface, which provides the surface charge. The solution of ψ, therefore, includes two terms, one is due to the bulk magnetic charge, the other one surface magnetic charge. The solution for $\psi_k(y)$ reads as follows: :

$$\begin{aligned}\psi_k(y) &= 4\pi i\left[e^{-kd/2}\cosh(ky) - 1\right]\left(\frac{k_x}{k^2}m_x(k) + \frac{k_z}{k^2}m_z(k)\right) &(2.52)\\ &\quad + 4\pi e^{-kd/2}\frac{\sinh(ky)}{k}m_y(k) &(2.53)\end{aligned}$$

Now we can calculate the dipolar interaction which is expressed in terms of $\mathbf{h}^{\rm dip}$ and $\mathbf{m}$:

$$H_D = -\frac{1}{2}\int dxdydz\mathbf{m}\cdot\mathbf{h}^{dip} \tag{2.54}$$

Explicitly,

$$H_D = -\frac{1}{2}\int\frac{dy}{d}\sum_{\mathbf{k}}[m_x(-\mathbf{k})h_x^{hip}(\mathbf{k},y) + m_y(-\mathbf{k})h_y^{hip}(\mathbf{k},y) + m_z(-\mathbf{k})h_z^{hip}(\mathbf{k},y)] \tag{2.55}$$

Substitute the expression of ψ in terms of $\mathbf{m}$, we have:

$$\begin{aligned}H_D = -\frac{1}{2}g^2\mu_B^2\frac{N}{V}\int\frac{dy}{d}\Big[\sum_{\mathbf{k}}4\pi\frac{e^{-kd/2}\cosh(ky) - 1}{k^2}\\ \Big(k_x^2 S^x(-\mathbf{k})S^x(\mathbf{k}) + k_x k_z S^x(-\mathbf{k})S^z(\mathbf{k}) + k_x k_z S^z(-\mathbf{k})S^x(\mathbf{k}) + k_z^2 S^z(-\mathbf{k})S^z(\mathbf{k})\Big)\end{aligned}$$

$$-\sum_{\mathbf{k}} 4\pi e^{-kd/2}\cosh(ky)S^y(-\mathbf{k})S^y(\mathbf{k})\Big]$$

where we transform the integral from real space to $\mathbf{k}$ space and we used the fact that due the definition of Fourier transformation for $\mathbf{m}$ and $\mathbf{S}_j$, we have $\mathbf{m}(\mathbf{r}) = g\mu_B\frac{N}{V}\mathbf{S}_j$ in real space, but $\mathbf{m}(\mathbf{k}) = g\mu_B(\frac{N}{V})^{1/2}\mathbf{S}(\mathbf{k})$ in k space. There are two terms $S^x(-\mathbf{k})S^z(\mathbf{k})$ and $S^z(-\mathbf{k})S^x(\mathbf{k})$ which contribute terms of linear a and three as.

Performing the integral over y, we have:

$$\begin{aligned}
H_D &= -\frac{1}{2}g^2\mu_B^2\frac{N}{V}4\pi\sum_{\mathbf{k}}\Big[(F_k-1)[k_x^2S^x(-\mathbf{k})S^x(\mathbf{k}) + k_z^2S^z(-\mathbf{k})S^z(\mathbf{k}) + k_xk_zS^x(-\mathbf{k})S^z(\mathbf{k}) \\
&\qquad + k_xk_zS^z(-\mathbf{k})S^x(\mathbf{k})]/k^2 - F_kS^y(-\mathbf{k})S^y(\mathbf{k})\Big] \\
&= \sum_{\mathbf{k}} f_1\left[S^+(-\mathbf{k})S^-(\mathbf{k}) + S^-(-\mathbf{k})S^+(\mathbf{k})\right] + f_2[S^+(-\mathbf{k})S^+(\mathbf{k}) + S^-(-\mathbf{k})S^-(\mathbf{k})] \\
&\quad + f_3S^z(-\mathbf{k})S^z(\mathbf{k}) + H^{(3)}
\end{aligned}$$

with

$$f_1 = \frac{\hbar\gamma 2\pi M}{S}\frac{1}{4}[(1-F_k)\sin^2\theta + F_k] \tag{2.56}$$

$$f_2 = \frac{\hbar\gamma 2\pi M}{S}\frac{1}{4}[(1-F_k)\sin^2\theta - F_k] \tag{2.57}$$

$$f_3 = \frac{\hbar\gamma 2\pi M}{S}(1-F_k)\cos^2\theta \tag{2.58}$$

and $H^{(3)}$ the 3 magnon terms:

$$H^{(3)} = \frac{\hbar\gamma 4\pi M}{4S}(1-F_k)\frac{k_xk_z}{k^2}[S^+(-\mathbf{k})S^z(\mathbf{k}) + S^z(-\mathbf{k})S^+(\mathbf{k}) + S^z(-\mathbf{k})S^-(\mathbf{k}) + S^-(-\mathbf{k})S^z(\mathbf{k})] \tag{2.59}$$

where we have defined $F_k = (1-e^{-kd})/kd$. $\hbar\gamma = g\mu_B$ and $M = g\mu_BNS/V$.

We can also calculate the dipole interaction by starting from the expression:

$$E_D = -\frac{\mu_0}{4\pi}\frac{3(\mathbf{m}_1\cdot\mathbf{e}_{12})(\mathbf{m}_2\cdot\mathbf{e}_{12})-\mathbf{m}_1\cdot\mathbf{m}_2}{r_{12}^3} \tag{2.60}$$

Or, written in Gaussian units:

$$E_D = -\frac{3(\mathbf{m}_1\cdot\mathbf{e}_{12})(\mathbf{m}_2\cdot\mathbf{e}_{12})-\mathbf{m}_1\cdot\mathbf{m}_2}{r_{12}^3} \tag{2.61}$$

$\mathbf{m}_{1,2}$ are the two magnetic moments. For a ferromagnet, we should define another quantity M which has a dimension of $[m]/[V]$ with V the volume.

$$\begin{aligned} H_D &= -\frac{1}{2}\int d\mathbf{r}_1 d\mathbf{r}_2 \frac{3(\mathbf{M}_1\cdot\mathbf{e}_{12})(\mathbf{M}_2\cdot\mathbf{e}_{12})-\mathbf{M}_1\cdot\mathbf{M}_2}{r_{12}^3} &(2.62)\\ &= \frac{1}{2}\int d\mathbf{r}_1 d\mathbf{r}_2 (\mathbf{M}_1\cdot\nabla_1)(\mathbf{M}_2\cdot\nabla_2)\frac{1}{r_{12}} &(2.63)\end{aligned}$$

where we have used $\nabla_i\nabla_j\frac{1}{r} = \frac{\delta_{ij}}{r} - \frac{3r_ir_j}{r^5}$.

Note that:

$$\begin{aligned} \frac{1}{r} &= \int \frac{d\mathbf{k}}{(2\pi)^3} e^{i\mathbf{kr}}\frac{4\pi}{k^2} &(2.64)\\ &= \frac{d}{V}\sum_{k_x,k_z}\int\frac{dk_y}{2\pi}e^{i\mathbf{kr}+ik_y y}\frac{4\pi}{k^2+k_y^2} &(2.65)\end{aligned}$$

where we have separated k_y from k_x and k_z, the latter two will be just denoted as $\mathbf{k}$. Then substitute the above Fourier transformation into the H_D, and use the Fourier transformation for M.

$$H_D = \frac{4\pi}{2}\sum_{\mathbf{k}}\int\frac{dy_1dy_2}{d}\int\frac{dk_y}{2\pi}M_i(-\mathbf{k})M_j(\mathbf{k})\frac{k_ik_j}{k^2+k_y^2}e^{ik_y(y_1-y_2)} \tag{2.66}$$

For the terms of $M_y(-\mathbf{k})M_y(\mathbf{k})$, we have:

$$\begin{aligned}
&\frac{4\pi}{2}\int\frac{dy_1dy_2}{d}\int\frac{dk_y}{2\pi}\frac{k_y^2}{k^2+k_y^2}e^{ik_y(y_1-y_2)}\\
&=\frac{4\pi}{2}\int\frac{dy_1dy_2}{d}[\delta(y_1-y_2)+\frac{ke^{k(y_1-y_2)}}{2}\theta(y1-y2)+\frac{ke^{k(y2-y1)}}{2}\theta(y2-y1)]\\
&=\frac{4\pi}{2}(1-\int\frac{dy_1dy_2}{d}[ke^{-k(y_1-y_2)}\theta(y1-y2)])\\
&=\frac{4\pi}{2}(1-(1-F_k))\\
&=\frac{4\pi}{2}F_k
\end{aligned}\tag{2.67}$$

Other terms can be calculated similarly, for example, the coefficient for M_xM_x is $\frac{4\pi}{2}(1-F_k)$.

2.3.3 Spectrum and Bogoliubov transformation

Together with expression for H_Z+H_{ex}, we can expand the total Hamiltonian in terms of a_k and $a_k^\dagger$. To the quadratic terms,

$$H_0=\hbar\sum_{\mathbf{k}}A_ka_k^\dagger a_k+\frac{1}{2}B_ka_ka_{-k}+\frac{1}{2}B_k^*a_k^\dagger a_{-k}^\dagger,\tag{2.68}$$

with

$$A_k= \quad [\gamma H_0+Dk^2+\gamma 2\pi M(1-F_k)\sin^2\theta+\gamma 2\pi MF_k]\tag{2.69}$$

$$B_k= \quad [\gamma 2\pi M(1-F_k)\sin^2\theta-\gamma 2\pi MF_k]\tag{2.70}$$

in which, $D=2JSa^2$, with a the lattice constant. $D=0.24\text{eV}\mathring{A}^2$. Note: $\gamma=g\mu_B/\hbar=2.8\text{GHz/kOe}$, 1eV$=2.4*10^5$Ghz.

We need to make the Bogoliubov transformation to obtain the dispersion relation.

$$a_k = u_k c_k + v_k c_{-k}^\dagger \tag{2.71}$$

$$a_k^\dagger = u_k c_k^\dagger + v_k^* c_{-k} \tag{2.72}$$

Here, $u_k = u_{-k}$ is chosen to be real, while $v_k = v_{-k} = |v_k|e^{-i\phi}$, whose phase should be determined by the phase of $B_k = |B_k|e^{i\phi}$.

$$|u_k^2| - |v_k^2| = 1 \tag{2.73}$$

$$u_k = (\frac{A_k + \omega_k}{2\omega_k})^{1/2} \tag{2.74}$$

$$v_k = e^{-i\phi}(\frac{A_k - \omega_k}{2\omega_k})^{1/2} \tag{2.75}$$

The magnon spectrum is:

$$\omega_k = (A_k^2 - |B_k|^2)^{1/2} \tag{2.76}$$

In Fig. 2.4, we show the magnon spectrum as a function of wave vectors with different angles θ for two different thicknesses of the film.

For the value of nonzero wavevector Q at the minimum energy point, we can calculate it by taking the derivative of $\omega(k)$ with respective to k and then set it to be zero. Specifically, Q satisfies:

$$(\gamma H_0 + DQ^2)\left(2DQ + m\frac{\partial F_k}{\partial k}\Big|_Q\right) + (\gamma H_0 + DQ^2 + mF_Q)2DQ = 0 \tag{2.77}$$

in which we define $m = \gamma 4\pi M$.

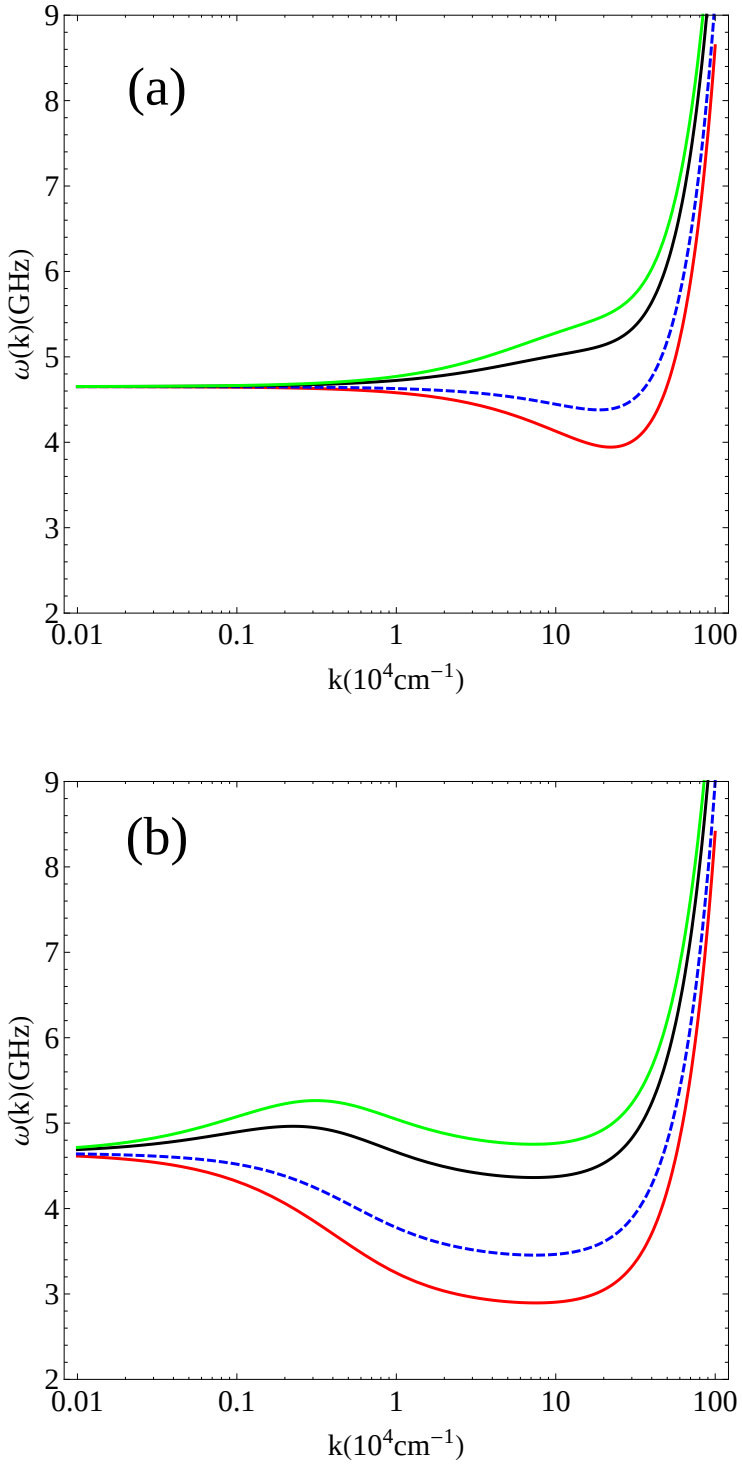

Figure 2.4: Dispersion relation of spin wave, $\omega_{\mathbf{k}}$, propagating with different directions. Respectively, $\theta = 0, \pi/6, \pi/3, \pi/2$ correspond to red, blue, black and green curves. The upper pabel corresponds to $d = 5.1$ μm, while the lower panel for $d = 0.1$ μm. In both cases, $H = 1.0$kOe.

In the case $H_0 \gg DQ^2$, if $Qd \gg 1$, we have $F_Q \sim \frac{1}{Qd}$, Q can be approximated as:

$$DQ^2 = \frac{m}{4Qd} \tag{2.78}$$

which gives:

$$Q \sim \left(\frac{m}{4Dd}\right)^{1/3} \tag{2.79}$$

Roughly it can be physically understood that Q corresponds to the point when the dipolar interaction equals to exchange interaction.

In the other limit, $Qd \ll 1$, we have $F_Q \sim 1 - \frac{Qd}{2}$,

$$DQ^2 = \frac{mQd}{4c} \tag{2.80}$$

with $c = 2 + \frac{m}{\gamma H_0}$ a constant. This gives:

$$Q = \frac{md}{4Dc} \tag{2.81}$$

For the dependence of Q on H_0, we first notice that if $H_0 = 0$, $Q = 0$. For a large H_0, that is, $H_0 \gg DQ^2$, Q is independent of H_0 for the case of Eq. 2.79, while for the case of Eq. 2.81, the dependence is also very weak.

In Fig. 2.5, we plot Q as a function of d and H, respectively. In (a), we plot Q as a function of d for $H_0 = 1$ kOe. We show the exact result by numerical calculation (red curve), and the approximation from Eq. 2.79 (Blue curve) and Eq. 2.81 (Green curve). In (b) and (c), we plot Q as a function of H_0 for $d = 5.1\mu$m and $d = 0.1\mu$m, respectively.

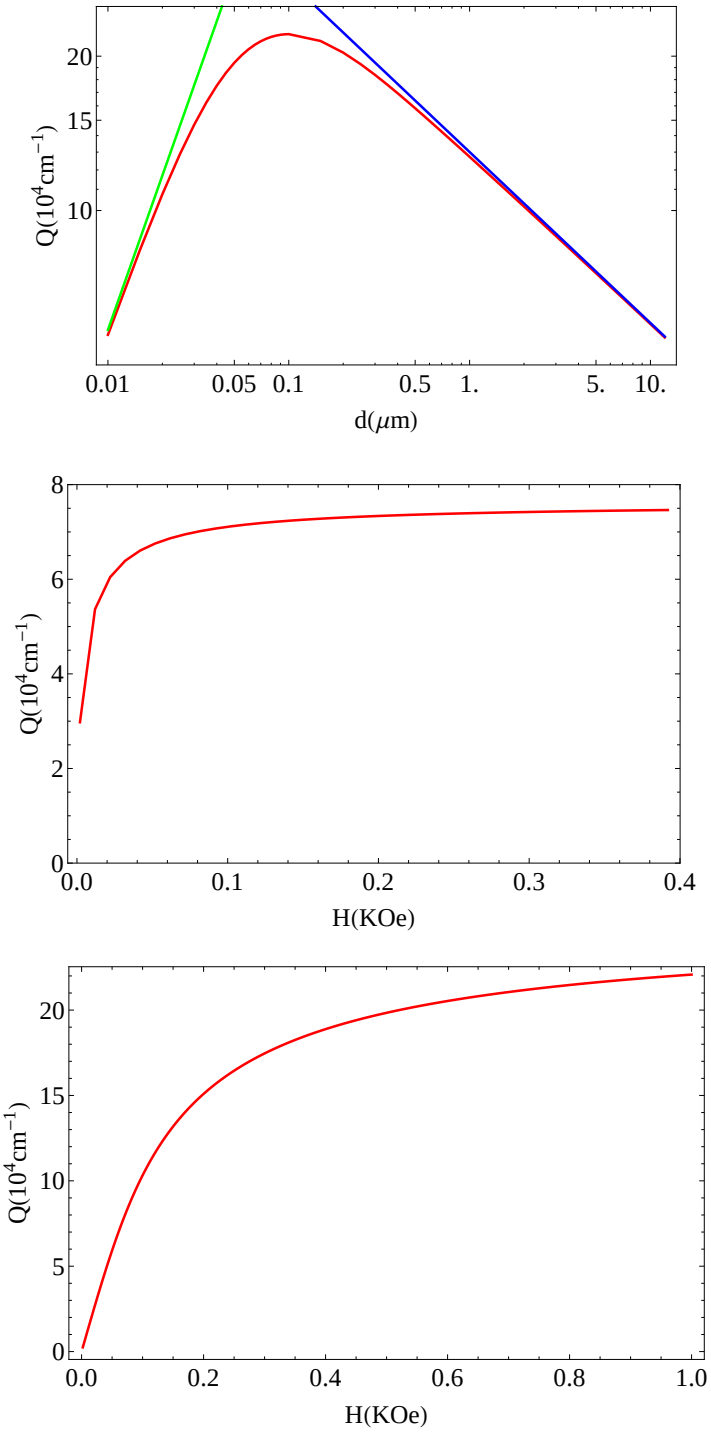

Figure 2.5: Nonzero wave vector Q at the minimum energy point as a function of thickness of film d (a), and as a function of external magnetic field H (b and c). In (a), $H = 1.0kOe$. We show the exact result by numerical calculation (red curve), and the approximation from Eq. 2.79 (Blue curve) and Eq. 2.81 (Green curve). In (b), $d = 5.1\mu$m. In (c) $d = 0.1$ μ m.

2.4 Experimental discovery of magnon condensation

2.4.1 YIG materials

Yttrium iron garnet (YIG) [11] is a ferrimagnetic material. As a kind of synthetic garnet, its chemical composition is written as $Y_3Fe_2(FeO_4)_3$, or $Y_3Fe_5O_{12}$. It has a complex cubic crystal structure with a lattice constant $a = 12.4\mathring{A}$. In each unit cell, there are 80 atoms containing 20 magnetic Fe^{+3} ions. 8 of the ions occupy the centers of octahedral, the other 12 are centered in tetrahedral sub-lattices. The octahedral and tetrahedral are antiferromagnetically coupled with each other. The Y^{3+} ions occupy all the dodecahedral sites. The iron ions in the two coordination sites exhibit different spins, giving rise to interesting magnetic behaviours. The Curie temperature of YIG is of 550 K. The saturated magnetization of YIG is 1.7 kOe.

YIG has a high Verdet constant. This results in unprecedented properties of YIG compared with other materials. For example, it has the narrowest ferromagnetic resonance line, generally smaller that 0.5 Oe. This means that the magnon lifetime in YIG is very long, of the order of few hundred nanoseconds, to the order of μs. Together with the slow magnon speeds (approximately four orders of magnitude slower than the speed of light), the spin-wave mean free paths is typically less than 10μm. In that sense, the low damping in YIG provides a spin-wave propagation to be observed on macroscopic scale. Moreover, YIG has high Q factor in microwave frequencies, low absorption of infrared wavelengths down to 600 nm, and very small linewidth in electron spin resonance. These properties find their wide applications microwave, optical, and magneto-optical applications, e.g. microwave YIG filters. Recently, YIG has been widely used in spin Seebeck effect.

2.4.2 Excitation and detection of magnons

2.4.2.1 Parallel pumping of magnons

Among different mechanisms to excite magnons, the parallel pumping is one of the most efficient and widely used [47]. By " parallel pumping", it means that the applied microwave magnetic field is oriented in the direction parallel to the inplane external static magnetic field H_0.The spatially uniform pumping field excites two magnons with the same frequency ω_p but with opposite wave vector $\pm\mathbf{k}_p$. It can be understood as the creation of two magnons by one photon in the pumping field. Assuming the microwave pumping field

$$\mathbf{h}(t) = h\cos(2\omega_p t)\hat{z} \tag{2.82}$$

due to Zeeman interaction, it gives an additional term in the Hamiltonian:

$$H' = -\gamma h\cos(2\omega_p t)\sum_{\mathbf{k}} a_{\mathbf{k}}^{\dagger}a_{\mathbf{k}} \tag{2.83}$$

where $a_{\mathbf{k}}$ and $a_{\mathbf{k}}^{\dagger}$ are the Bosonic operators derived from the Holstein Primakoff transformation.

As shown in the above section, the existence of dipolar interaction produces non-diagonal terms in the quadratic Hamiltonian of $a_{\mathbf{k}}$ and $a_{\mathbf{k}}^{\dagger}$. One must perform the Bogoliubov transformation to diagonalize Hamiltonian. Therefore, in terms of $c_{\mathbf{k}}$ and $c_{\mathbf{k}}^{\dagger}$, we have terms like

$$\gamma h\cos(2\omega_p t)\sum_{\mathbf{k}}\frac{|B_k|}{\omega_k}\left[c_{\mathbf{k}}^{\dagger}c_{-\mathbf{k}}^{\dagger} + h.c.\right] \tag{2.84}$$

This correspond to the creation and annihilation of $(\mathbf{k}, -\mathbf{k})$ magnon pairs. The

essential feature of this relaxation process is that it is nonlinear. That it, the rate at which energy flows from microwave pumping field into the excited magnon pairs depends on the occupation number $\langle n_{\mathbf{k}} \rangle$, which, in turn, depends upon the amplitude of the driving field, as well as on the relaxation rate $\eta_{\mathbf{k}}$. Only if the driving rate exceeds the relaxation rate, the excited magnons can increase. The threshold for this process is given by

$$h_{\text{crit}} = \min \left(\frac{4\omega_p \eta_{\mathbf{k}}}{\gamma \omega_M \sin^2 \theta_{\mathbf{k}}} \right) \tag{2.85}$$

where min means that we use that value of $\mathbf{k}$ giving the minimum.

2.4.2.2 Detection of magnon kinetics: Briouloin light scattering

Detecting spin waves with sufficient resolution can provide us the information of dynamics of spin waves and henceforth, the information of interactions of spin waves and the relaxation rate and macroscopic parameters of the magnetic media. Several different techniques have been developed for this purpose, e.g. the neutron scattering. The most recently developed Brillouin Light scattering method based on the inelastic scattering of light from magnons, has many advantages and find its wide application in the GHz regime [75, 74].

In BLS, the photon with frequency ω_i and wave vector k_i interacts with a magnon with frequency ω_m and wave vector k_m. The magnon can be absorbed or emitted by the photon whose energy is correspondingly increased or decreased:

$$\hbar\omega_m = \hbar\omega_i \pm \hbar\omega_s \tag{2.86}$$

$$\hbar\mathbf{k}_m = \hbar\mathbf{k}_i \pm \hbar\mathbf{k}_s \tag{2.87}$$

are the conservations of energy and momentum, respectively. $\pm$ denotes the absorb-

tion (emission) of a magnon.

The scattered light with increased (decreased) frequency are called Stokes (Anti-Stokes). Its intensity is proportional to the number density of magnons at state $\mathbf{k}_m$ with frequency $\omega_{\mathbf{k}}$. Therefore, by analyzing the scattered light, the information of frequency, wave vector and density of magnons can be determined at the same time.

Since the BLS is an optical method, it can reach very high resolution. Nowadays, the temporal resolution can be as high as the order of ~ 1 ns. Its spatial resolution, restricted by the laser beam focus, is of the order of 50μm.

2.4.3 Discovery of magnon BEC and confirmation of coherence

The magnon BEC was first discovered in 2006 by the group of Demokritov [21]. A series of subsequent work confirmed this discovery and proposed more questions [27, 22, 26, 28, 76].

2.4.3.1 Experimental discovery

The experimental set-up for magnon excitation in YIG films and their detection using Brillouin light scattering (BLS) spectroscopy is shown schematically in Fig. 2.6 . The thickness of YIG film is 5 μm. The film is placed in a uniform static magnetic field, H, up to 1 kOe. The low frequency part of the spectrum of the magnons with wave vectors parallel to the static magnetization is shown by the solid line in the log-log plot. As can be seen, two minima exist in this spectrum. A microwave photon with a frequency of $2\nu_p$ creates two primary excited magnons of frequency ν_p and opposite wavevectors. These primary magnons relax very fast and create a quasi-equilibrium distribution of thermalized magnons, forming the quasiequilibrium magnon gas described by

$$n(\nu) = \frac{1}{\exp(\frac{h\nu-\mu}{k_B T_0}) - 1} \tag{2.88}$$

with μ the effective chemical potential and T_0 the effective temperature. In the experiment, one found that T_0 is almost unchanged while μ has a significant change as delay after the pumping increases, and finally μ reaches the minimum energy of the spectrum which leads to Bose-Einstein condensation.

To examine the distribution of the magnons over the spectrum, Brillouin light scattering spectroscopy was used. As shown in Fig. 2.6, the incident laser beam is focused onto the resonator. The beam passes through the YIG film, is reflected by the resonator, and passes through the film again. Then the light is collected by a wide-aperture objective lens and sent to the interferometer for frequency analysis of light photons inelastically scattered by the magnons. This approach allows a simultaneous detection of the magnons in a wide interval of the in-plane wavevectors, estimated as $\pm 2 \times 10^5$ cm^{-1}, which exceeds km. as indicated by the red hatching in Fig. 2.6. The time evolution of $n(\nu)$ after the start of pumping is determined using time frames of 100 μm width.

The BLS results can be fitted based on Eq. 2.88 with the chemical potential being a fitting parameter (The temperature T_0 is almost a constant). At different delay times and different pumping power, BLS spectra show different behaviors, see Fig. 2.7. For $P = 4.0$ W, the data cannot be described using the Bose-Einsterin statistics, illustrating that the thermalization process at those magnon densities lasts more than 200 ns. By contrast, the data for the pumping power $P = 5.9$ W are described very well by the Bose-Einsterin statistics at room temperature and a non-zero chemical potential μ, $\mu/k_B = 98$ mK. It is seen that the chemical potential increases with time, reflecting the growth of the magnon density caused by the pumping. After about 400ns, the chemical potential increases to the minimum energy and can no longer increase. The BLS spectra can be fitted with Eq. 2.88 plus a delta function at ν_m. The amplitude of this delta function increases with time until the switch-off

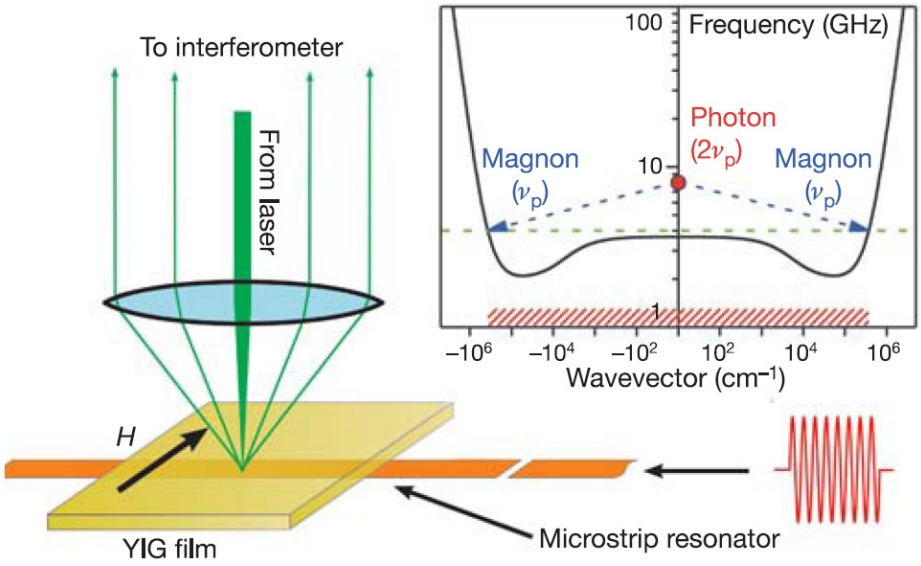

Figure 2.6: The set-up for magnon excitation and detection. The pumping microwave pulse is sent through the resonator. The laser beam is focused onto the resonator, and the scattered light is directed to the interferometer. The inset shows the parallel pumping due to the microwave pulse. One photon of frequency $2\nu_p$ excites two magnons with same frequency ν_p. The low-frequency part of the magnon spectrum is shown by the solid line. The wavevector interval indicated by the red hatching corresponds to the interval of the wavevectors accessible for Brillouin light scattering (BLS). Figure is taken from Ref.[21]

of pumping pulse. This is the first experimental verification of magnon BEC.

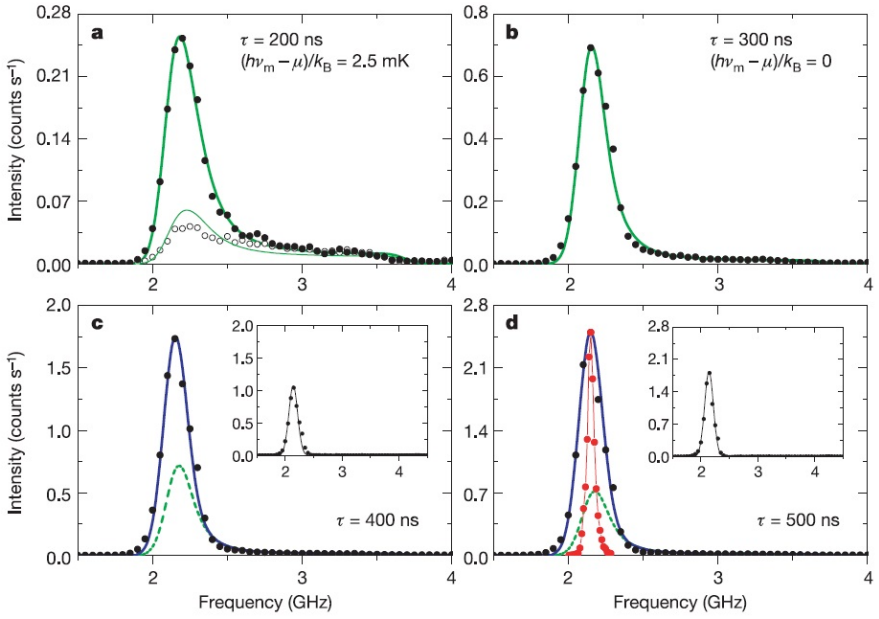

Figure 2.7: The fitting of BLS intensity using Eq. 2.88 for different pumping power at different delay times after the start of pumping. Figure is taken from Ref.[21]

Further experiments in the same group are done to explore this new phenomena. In 2007, Demidov *et al* [18, 19] showed a more clear picture of the thermalization of the Boson gases, see Fig. 2.8. It was shown that the relaxation of primary magnons into the magnons with smaller energies happens through the multiple magnon-magnon scattering events, and therefore, the magnons reaching the bottom of the spectrum lose the initial phase coherence, which might be introduced by the external pumping source. It was also shown that the speed of the thermalization depends on the density of the injected magnons, i.e. on the pumping power.

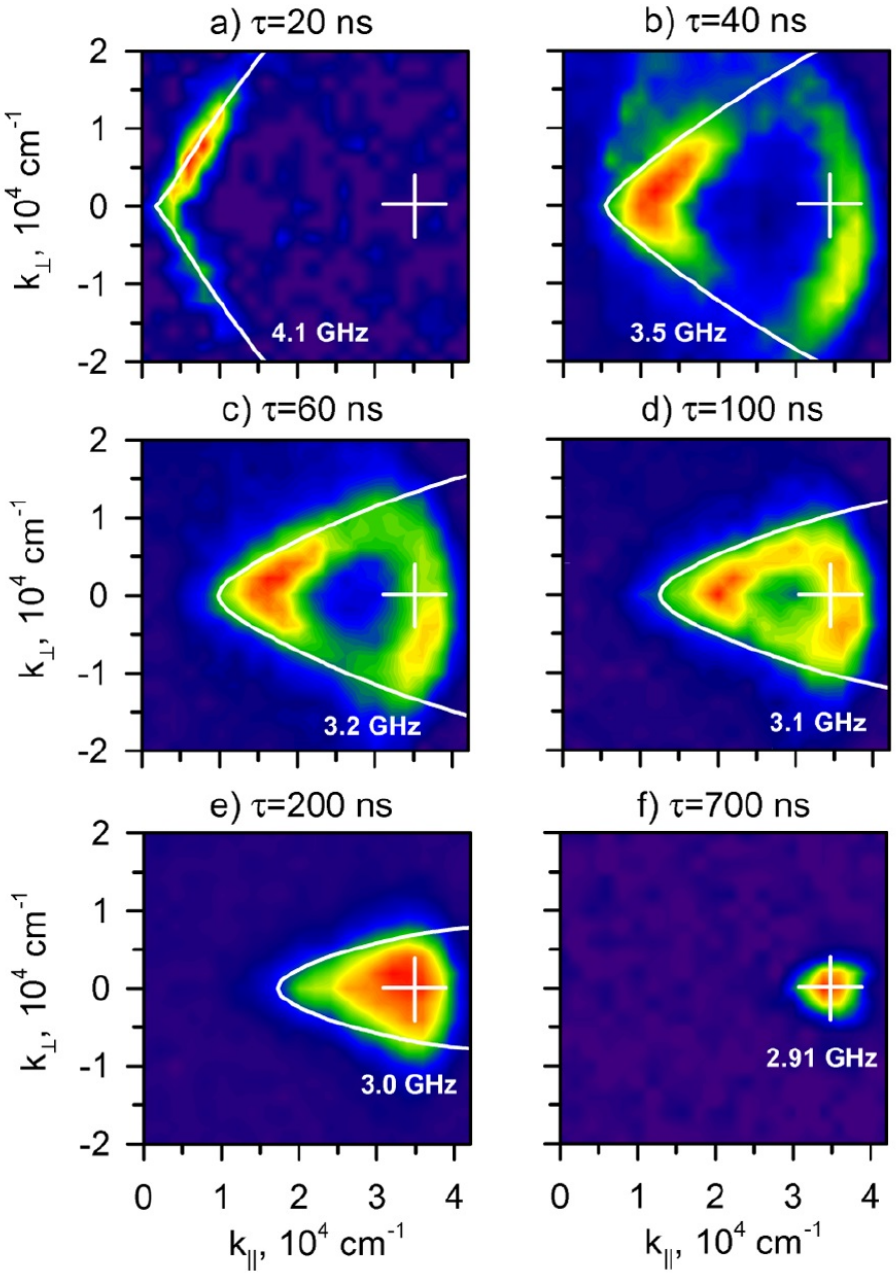

Figure 2.8: The BLS intensity in the phase space for different delay times after the start of pumping. The relaxation of primary magnons into the magnons with smaller energies is clearly shown. Figure is taken from Ref.[18]

2.4.3.2 Spontaneous coherence and magnon kinetics

After the discovery of magnon BEC, Snoke [80] asked the question whether the observed phenomena is really a realization of BEC. He proposed three questions: Firstly, it was long time ago proved that in exactly 2D system, there would be no real Bose-Einstein Condensation. Secondly, since the particles are quasiparticles with finite life time, the system is not in equilibrium. Thirdly, the driving field is itself coherent, which would drive the system to be in coherent state. Rather using the term BEC, Snoke adopts another term: spontaneous coherence to describe a generalized system. This spontaneous coherence can occur in two-dimensional systems just as well as in three dimensions. Experiments with liquid helium on surfaces, for example, have shown that two-dimensional helium can be superfluid, just like bulk helium. The only difference in 2D and 3D is that in 2D, the fluctuation is so strong that the coherence length is reduced to be finite. Therefore for a finite 2D system, the first problem becomes no longer a problem. For the second problem, as long as the life time of quasiparticle is much longer than the thermalization time between quasiparticles, the system can reach a quasiequilibrium state, and the condensation can occur. The most important problem here is the coherence. Condensation into the lowest quantum level is enough. One needs to show direct evidence of coherence and also that the coherence is spontaneous, not due to external coherent driving field.

Since the spontaneous emergence of coherence is an obligatory manifestation of BEC, the existence of room temperature BEC was then further illustrated by the experiment done by Demidov *el al* [20] in 2008 by using a short microwave pumping pulse instead of continuous driving. The duration of short pulse is 30 ns, much smaller than the characteristic thermalization time in the magnon gas. Consequently, the

processes of magnon redistribution over the spectrum and the formation of BEC were studied in a magnon gas, which was free from any influence of the external driving force. Moreover, by exploring the decay time of magnons located at the minimum frequency at different pumping power, the experiments show two different decaying rate before and after the appearance of BEC (Fig. 2.9). The BLS intensity is proportional to the temporal average of the square of the electric field of the scattered light, E. In the case of many scatters, the total scattering intensity is proportional to $\langle(\sum E_i)^2\rangle$, where E_i is the scattered field of the ith scatter. If the scatters are incoherent, the total scattering intensity would be $\propto \langle\sum E_i^2\rangle$. Therefore, the temporal dependence of the BLS intensity would be the same as that of the decay of each magnon density $\propto \exp(-\alpha t)$. However, for the coherent scatters, the scattering intensity is proportional to $\propto N^2\langle E_i^2\rangle$, correspondingly, the decay of BLS intensity would follow $[\exp(-\alpha t)]^2 = \exp(-2\alpha t)$. In summary, the BLS intensity decays twice as fast for coherent magnons than that for incoherent magnons.

Bose-Einstein condensation of magnons under incoherent pumping was also studied [13]. In the experiments, the magnon excitation is pumped by a noise pumping covering the frequency interval $f_p \pm \Delta f/2$. It turns out that the pumping power threshold increases from the original $(\delta f_p)^2$ to $\delta f_p(\delta f_p + \Delta f)$, where δf_p is the magnon relaxation frequency. The BEC is verified by detecting the electromagnetic radiation from the excited system.

2.4.3.3 Current theoretical studies.

There appear a lot of theoretical work trying to explore magnon BEC observed in the experiments [32, 31]. In 2008, Tupitsyn *et al* [85] studied the stability of the magnon BEC system and found that due to the strong dependence of magnon-magnon interaction on the external magnetic field orientation, the magnon BEC in

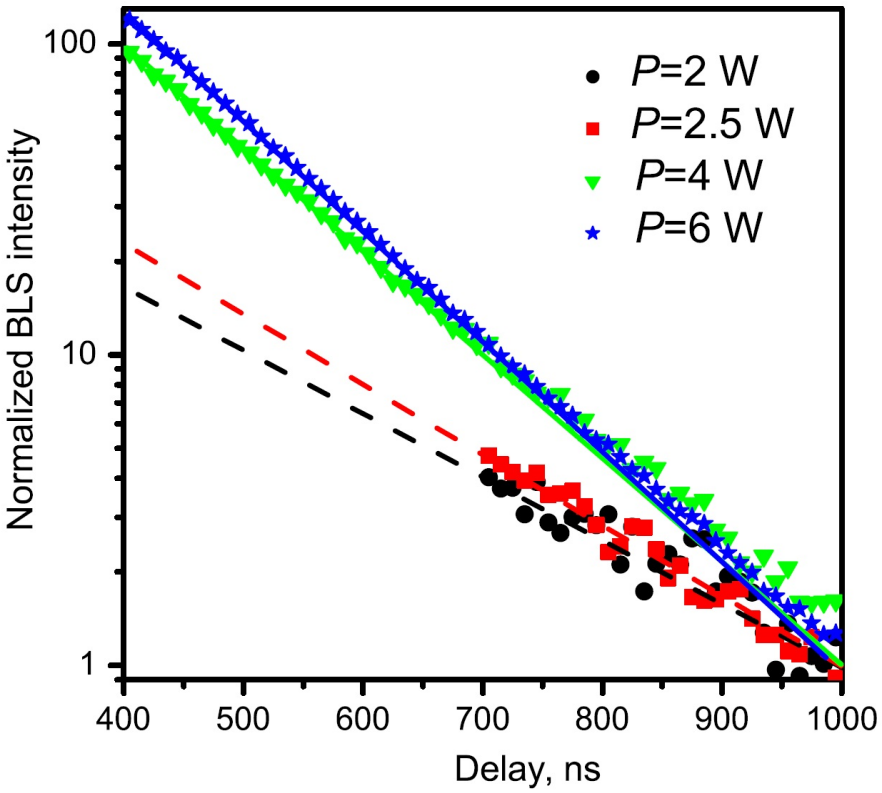

Figure 2.9: The BLS intensity of the magnons located at the minimum energies as a function of time. It reveals the decay of magnons with lowest energy. For condensed and non-condensed magnons, the decays show different rate. Figure is taken from Ref.[20]

current experiments is unstable. They further propose that by applying a strong external magnetic field in the perpendicular direction to obtain a repulsive magnon-magnon interaction, a high-density magnon BEC would be achieved.

A Ginzburg-Landau model was proposed to study the magnon Bose-Einstein condensation [58] presumably assuming equal number of condensed magnons in the two minima. They incorporate the effect of pumping field by introducing a δ function into the equation and introduce phenomenologically the interactions between the two magnon condensates. They found that there are symmetric and asymmetric solutions and both of which are stable.

In the papers of Rezende [70, 71, 72], he also provides some studies on the dynamics of the magnon system. He pointed out that the wave function of the magnon condensate in configuration space satisfies a Gross-Pitaevskii equation similarly to other BEC systems. He also studies the appearance of spontaneous coherence for the magnon system under excitations by microwave pumping. He shows that if the microwave driving power exceeds a threshold value the nonlinear magnetic interactions create cooperative mechanisms for the onset of a phase transition leading to the spontaneous generation of quantum coherence and magnetic dynamic order in a macroscopic scale. However, Rezende's study also assumes that the condensed magnons distribute equally between the two minima.

By calculating the interactions of magnons in YIG film, Troncoso and Nunez [84] also studied the spontaneous coherence of the system, and some related problems, like internal Josephson effect and appearance of interference pattern and vortices. However, the distribution of magnons in the two minima is not discussed.

3. SPONTANEOUS BREAKING OF MIRROR SYMMETRY BREAKING IN MAGNON BEC

3.1 Motivation and introduction

Bose-Einstein condensation (BEC), one of the most intriguing macroscopic quantum phenomena, has been observed in equilibrium systems of Bose atoms, like ^{4}He [42, 1], ^{87}Rb [4] and ^{23}Na [17]. Recent experiments have extended the concept of BEC to non-equilibrium systems consisting of photons [46] and of quasiparticles, such as excitons [10], polaritons [43, 5, 2] and magnons [8, 21]. Among these, BEC of magnons in films of Yttrium Iron Garnet (YIG), discovered by the group of Demokritov [21, 27, 19, 20, 18, 26, 25, 28, 66], is distinguished from other quasiparticle BEC systems by its room temperature transition and two-dimensional anisotropic properties.

The peculiarity of the spin-wave energy spectrum of a YIG film in an external inplane magnetic field is that, it has two energetically degenerate minima. Therefore it is possible that the system may have two condensates in momentum space [52]. An experiment by Nowik-Boltyk *et al.* [66] indeed shows a low-contrast spatial modulation pattern, indicating that there is interference between the two condensates. The details of this experiment are shown in Fig. 3.1. In their paper, the low-contrast is explained qualitatively by the idea that the strength of phase locking between the two condensates are decreased because only a small part of the magnons are condensed. However, this explanation is not satisfactory.

Current theories [85, 71, 70, 72, 58, 84] do not describe the appearance of coherence or the distribution of the two condensates. Our theory agrees well with the experiment, and we predict a new kind of collective oscillation, called zero sound.

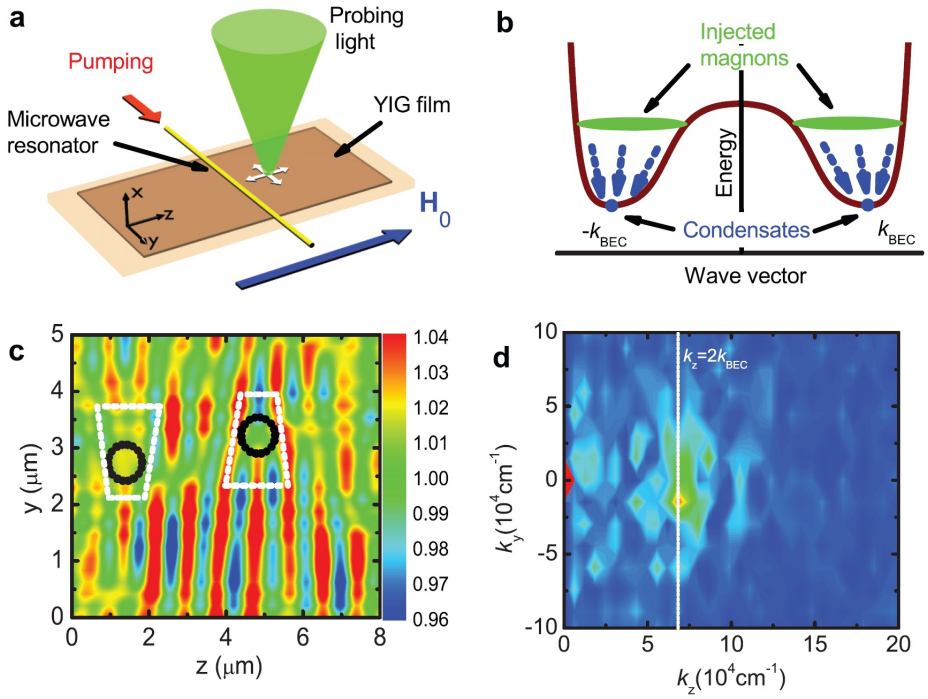

Figure 3.1: Schematic of the experiment setup and results of two-dimensional imaging of the interference pattern. (a) Experimental setup. (b) Schematic of magnon spectrum along the direction of magnetic film. It shows two degenerate spectral minima with non-zero wave vectors k_{BEC}. (c) Measured BLS intensity in the real space. Dashed circles show the positions of topological defects. (d) Fourier transform of the measured spatial map. Dashed line marks the value of the wave vector equal to $2k_{\mathrm{BEC}}$. Figure is taken from Ref.[66].

In this section, we point out that a complete description of BEC in microwave-pumped YIG films must account for the 4th order interactions, including previously neglected magnon-non-conserving terms originating in the dipolar interactions. The theory explains not only the appearance of coherence but also quantitatively explains the low contrast of the experimentally observed interference pattern. Moreover, our theory predicts that, on increasing the film thickness from a small value d, there is a transition from a high-contrast symmetric phase for $d < d_c$, with equal numbers of condensed magnons filling the two minimum states, to the low-contrast coherent non-symmetric phase for $d > d_c$, with different numbers of condensed magnons filling the two minimum states. In comparatively thin films ($d < 0.2\mu$m) the same transition can be driven by an external magnetic field H. At another critical thickness $d^* > d_c$, the sum of phases of the two condensates changes from π to 0; at this transition point the system is in a completely non-symmetric phase with only one condensate, for which there is no interference. In the experiment of Ref.[66] the thickness of film was larger than d^*. We suggest that the phase transitions may be identified by measuring the contrast of the spatial interference pattern for various d and H. We also predict a new type of collective magnetic oscillation in this system and discuss the possibility of domain walls in non-symmetric phases.

3.2 Number of condensed magnons $N_c = N_Q + N_{-Q}$

Experimentally, the spin lattice relaxation time is of order 1 μs, whereas the magnon-magnon thermalization time is of order 100 ns; the magnons are long-lived enough to equilibrate before decaying, thus making BEC possible [21]. After the thermalization time the pumped magnons go to a quasi-equilibrium state with a non-zero chemical potential μ. The number of pumped magnons $N_p = N(T,\mu) - N(T,0)$, where $N(T,\mu) = V\sum_{\mathbf{k}} \frac{1}{e^{(\omega_k-\mu)/T}-1}$, is determined by the pumping power and the

magnon lifetime. μ is a monotonically increasing function of N_p but cannot exceed the energy gap Δ_0. Therefore, on further increase of pumping some of the pumped magnons fall into the condensate. The equation $N_p = N(T, \Delta_0) - N(T, 0)$ thus defines the critical line of condensation. Since $\Delta_0 \ll T$ and $N_p \ll N(T, 0)$ this equation can be satisfied at a rather high temperature. The total number of condensed particles is [21, 9]

$$N_c = N_p - N(T, \Delta_0) + N(T, 0) \tag{3.1}$$

In exactly 2D systems BEC formally does not exist since in the continuum approximation the sum in $N(T, \mu)$ diverges. However, at strong enough pumping the chemical potential approaches exponentially close to the energy gap: $\Delta_0 - \mu \approx \Delta_0 \exp(-N_p/N_0)$, where $N_0 = VTm/\hbar^2$. At $N_p/N_0 > \ln(T/\Delta_0)$ all pumped magnons occupy only one or two states $\pm Q$.

Eq.(3.1) determines only the total number of particles in the condensate. The distribution of the condensate particles between the two minima remains undetermined in the quadratic approximation. To resolve this issue it is necessary to consider the fourth order terms in the Holstein-Primakoff expansion of the exchange and dipolar energy. Terms of third order in this expansion occur due to the dipolar interaction, but they vanish for the condensate values of momentum $(0, \pm Q)$ since in the third order the total momentum cannot be zero.

3.3 Magnon interaction

Following the same procedure as in Section 2, we calculate the interactions between magnons.

The third order term, that is, the three magnon term, is given by $H^{(3)}$:

$$H^{(3)} = f_0 \sum_{\mathbf{k},q} [a_k^\dagger a_q^\dagger a_{q+k} + a_{q+k}^\dagger a_q a_k] \tag{3.2}$$

with

$$f_0 = \frac{\hbar\gamma 4\pi M}{\sqrt{2SN}}(F_k - 1)\sin\theta\cos\theta \tag{3.3}$$

F_k is the form factor defined as: $F_k = \frac{1-e^{-kd}}{kd}$.

Using the Bogoliubov transformation, operator a is transformed to normal mode described by operator c. Considering the symmetry of $u_k = u_{-k}$, $v_k = v_{-k}$ and $f_0(k)f_0(-k)$, we have:

$$\begin{aligned} H^{(3)} &= f_0\Big[a_1[c_k^\dagger c_q^\dagger c_{k+q} + c_{k+q}^\dagger c_k c_q] + a_2[c_k^\dagger c_{k+q} c_{-q} + c_{k+q}^\dagger c_{-q}^\dagger c_k] \\ &\quad + a_3[c_k^\dagger c_q^\dagger c_{-(k+q)}^\dagger + c_k c_q c_{-(k+q)}]\Big] \end{aligned} \tag{3.4}$$

with

$$a_1 = u_k u_q u_{k+q} + v_k u_q u_{k+q} + u_k v_q v_{k+q} + v_k v_q v_{k+q} \tag{3.5}$$

$$a_2 = u_k v_q u_{k+q} + v_k u_q v_{k+q} \tag{3.6}$$

$$a_3 = u_k u_q v_{k+q} + u_k v_q v_{k+q} \tag{3.7}$$

We can further simplify by writing just:

$$H^{(3)} = C[c_k^\dagger c_q^\dagger c_{k+q} + c_{k+q}^\dagger c_k c_q] + C'[c_k^\dagger c_q^\dagger c_{-(k+q)}^\dagger + c_k c_q c_{-(k+q)}] \tag{3.8}$$

with

$$\begin{aligned} C(k,q) &= f_0(k)[u_k u_q u_{k+q} + v_k u_q u_{k+q} + u_k v_q v_{k+q} + v_k v_q v_{k+q}] \\ &+ f_0(k+q)[u_{k+q} v_q u_k + v_{k+q} u_q v_k] \end{aligned} \tag{3.9}$$

and $C' = f_0(k)a_3$ Third order interaction, or the three magnon process, doesn't affect the formation of BEC, but is important in the relaxation of magnons.

The fourth order interacting part, in terms of operators $a_{\mathbf{k}}$ and $a^{\dagger}(\mathbf{k})$, has the form:

$$\begin{aligned} H_{int}^{(4)} &= -\sum_{\mathbf{k}} \frac{f_2(k)}{N} \sum_{q,q'} (a^{\dagger}_{q+q'+k} a_q a_{q'} a_k + h.c.) \\ &+ \sum_{\mathbf{k}} \left(\frac{D_k + f_3(k) - D_q - 2f_1(q)}{2N} \right) \sum_{q,q'} [a^{\dagger}_{q+k} a^{\dagger}_{q'-k} a_q a_{q'} + h.c.] \end{aligned} \tag{3.10}$$

in which

$$f_1 = \frac{\hbar\gamma 2\pi M}{S}[(1 - F_k)\sin^2\theta + F_k]/4 \tag{3.11}$$

$$f_2 = \frac{\hbar\gamma 2\pi M}{S}[(1 - F_k)\sin^2\theta - F_k]/4 \tag{3.12}$$

$$f_3 = \frac{\hbar\gamma 2\pi M}{S}(1 - F_k)\cos^2\theta \tag{3.13}$$

$$D_k = -J\sum_{\delta} e^{i\mathbf{k}\cdot\delta} = \frac{D}{2S}k^2 - zJ \tag{3.14}$$

3.3.1 In the vicinity of minimum energy

The above expressions for the interactions of magnons are too complicated. Since we are only interested in the condensed magnons in the lowest energy level, we can extract the interactions of the condensed magnons only. In the vicinity of minimum energy with $k = \pm Q$, we have:

$$\begin{aligned} H_{\text{int}} &= -[a^{\dagger}_Q a^{\dagger}_Q a_Q a_Q + a^{\dagger}_{-Q} a^{\dagger}_{-Q} a_{-Q} a_{-Q}]\Big[\frac{DQ^2}{2S} + \frac{\hbar\omega_M}{8S} 2F_Q\Big]/N \\ &\quad -a^{\dagger}_Q a^{\dagger}_{-Q} a_{-Q} a_Q \Big[-4\frac{DQ^2}{2S} + \frac{\hbar\omega_M}{8S} 8F_Q - \frac{\hbar\omega_M}{2S} 2(1 - F_{2Q})\Big]/N \end{aligned}$$

$$+[a_Q^\dagger a_Q a_Q a_{-Q} + a_{-Q}^\dagger a_{-Q} a_{-Q} a_Q + h.c.]\frac{\hbar\omega_M}{8S}3F_Q/N \tag{3.15}$$

where we denote $\omega_M = \gamma 4\pi M$.

The a_k should be replaced by c_k using the Bogoliubov transformation. The 4-th order interaction of condensate amplitudes reads

$$\begin{aligned}\hat{V}_4 \quad &= A[c_Q^\dagger c_Q^\dagger c_Q c_Q + c_{-Q}^\dagger c_{-Q}^\dagger c_{-Q} c_{-Q}] \\ &+2Bc_Q^\dagger c_{-Q}^\dagger c_{-Q} c_Q \\ &+C[c_Q^\dagger c_Q c_Q c_{-Q} + c_{-Q}^\dagger c_{-Q} c_{-Q} c_Q + h.c.].\end{aligned} \tag{3.16}$$

where, $c_{\pm Q}$ and $c_{\pm Q}^\dagger$ are the annihilation and creation operators for magnons in the two condensates located at the two energy minima $(0, \pm Q)$ in the 2-D momentum space The coefficients in Eq.(3.16) are:

$$\begin{aligned}A = \quad &-\frac{\hbar\omega_M}{4SN}[(\alpha_1 - \alpha_3)F_Q - 2\alpha_2(1 - F_{2Q})] \\ &-\frac{DQ^2}{2SN}[\alpha_1 - 4\alpha_2], \\ B = \quad &\frac{\hbar\omega_M}{2SN}[(\alpha_1 - \alpha_2)(1 - F_{2Q}) - (\alpha_1 - \alpha_3)F_Q] \\ &+\frac{DQ^2}{SN}[\alpha_1 - 2\alpha_2], \\ C = \quad &\frac{\hbar\omega_M}{8SN}[(3\alpha_1 - \frac{20}{3}\alpha_3 + 3\alpha_2)F_Q \\ &+\frac{16}{3}\alpha_3(1 - F_{2Q})] + \frac{DQ^2}{SN}\alpha_3,\end{aligned} \tag{3.17}$$

with $\alpha_1 = u^4 + 4u^2v^2 + v^4$, $\alpha_2 = 2u^2v^2$ and $\alpha_3 = 3uv(u^2 + v^2)$. Here, u and v are the coefficients of Bogoliubov transformation Here, u and v are the coefficients of Bogoliubov transformation (see the Methods section for details). $S = 14.3$ is the effective spin, N the total number of spins in the film, M the magnetization and

$\hbar\omega_M = \gamma 4\pi M$ with gyromagnetic ratio $\gamma = 1.2 \times 10^{-5}$eV/kOe. D is proportional to exchange constant and $F_k = (1 - e^{-kd})/kd$. Similar results for the coefficients A and B were obtained in Ref.[85]. Coefficient C, which violates magnon number conservation, was not considered previously. Below we show that C is the only source of coherence between the two condensates. The three coefficients A, B and C, whose values as functions of H are shown in Fig.3.2 for two typical values of d, determine the distribution of condensed magnons in the two degenerate minima. Ref.[85] assumed a symmetric phase with condensed magnons in both minima having equal amplitudes and equal phases. Later, Ref.[71] assumed filling of only one minimum. More recently Ref.[84] considered Josephson-like oscillations by starting from two condensates with equal numbers of magnons but different phases. Our theory predicts coherent condensates and the ratio of their amplitudes without any additional assumption.

Notice that the minimum point Q can be estimated by $\frac{\hbar\omega_M}{Qd} = DQ^2$, which gives $Q \sim (\frac{\hbar\omega_M}{Dd})1/3$. For $d = 5\mu m$, we have $Q \sim 10^5 cm^{-1}$. $Qd \sim 50 \ll 1$.

3.4 Symmetry breaking of mirror symmetry

Coefficient C, which violates magnon number conservation, was not considered previously. Below we show that C is the only source of coherence between the two condensates. The three coefficients A, B and C, whose values as functions of H are shown in Fig.3.2 for two typical values of d, determine the distribution of condensed magnons in the two degenerate minima. Ref.[85] assumed a symmetric phase with condensed magnons in both minima having equal amplitudes and equal phases. Later, Ref.[71] assumed filling of only one minimum. More recently Ref.[84] considered Josephson-like oscillations by starting from two condensates with equal numbers of magnons but different phases. Our theory predicts coherent condensates

and the ratio of their amplitudes without any additional assumption. In terms of condensate numbers $N_{\pm Q}$ and phases $\phi_{\pm}$, the condensate amplitudes are $c_{\pm Q} = \sqrt{N_{\pm Q}}e^{i\phi_{\pm}}$. Substituting them into eq.(3.16) we find:

$$\begin{aligned} V_4 = \quad & A(N_Q^2 + N_{-Q}^2) + 2BN_Q N_{-Q} \\ & +2C\cos\Phi(N_Q^{\frac{3}{2}}N_{-Q}^{\frac{1}{2}} + N_Q^{\frac{1}{2}}N_{-Q}^{\frac{3}{2}}), \end{aligned} \tag{3.18}$$

where we introduce the total phase $\Phi = \phi_+ + \phi_-$. To minimize this energy, Φ must equal π for $C > 0$ and must equal 0 for $C < 0$. Fig.3.2 shows that the sign of C changes for different d and H, which indicates a transition of Φ between 0 and π. For both $C > 0$ and $C < 0$ a coherence between the two condensate amplitudes is established. In contrast to the Josephson-like interaction, the sum rather than the difference of the two condensate phases is fixed.

Since the total number of condensed magnons $N_c = N_Q + N_{-Q}$ is uniquely determined by the pumping (see Methods), the energy is minimized only by the so far unspecified difference $\delta = N_Q - N_{-Q}$. In terms of N_c and δ the condensate energy eq.(3.18) is:

$$V_4 = \frac{1}{2}\Big[(A+B)N_c^2 - (B-A)\delta^2 - 2|C|N_c\sqrt{N_c^2 - \delta^2}\Big]. \tag{3.19}$$

The ground state of the condensates depends on the criterion parameter:

$$\Delta = A - B + |C|. \tag{3.20}$$

When $\Delta > 0$, $\delta = 0$ minimizes the energy, so the two minima are filled with equal number of condensed magnons. This is the symmetric phase with $N_Q = N_{-Q}$. When $\Delta < 0$, the minimum shifts to $\frac{\delta^2}{N_c^2} = 1 - \frac{C^2}{(B-A)^2}$. This is the non-symmetric

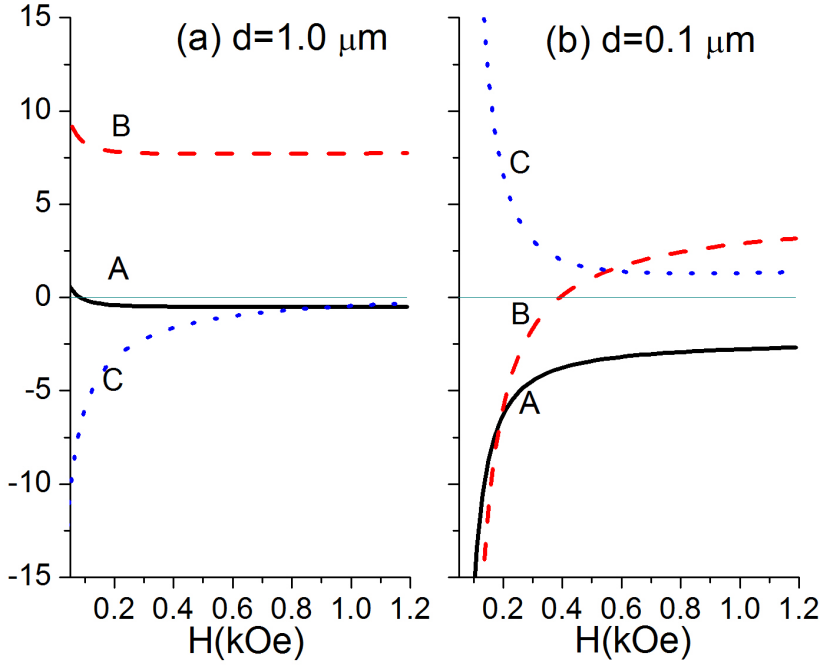

Figure 3.2: The interaction coefficients A, B and C (in units of mK/N, with N the total number of spins in the film) as a function of magnetic field H for film thickness (a) $d = 1.0$ μm and (b) $d = 0.1$ μm.

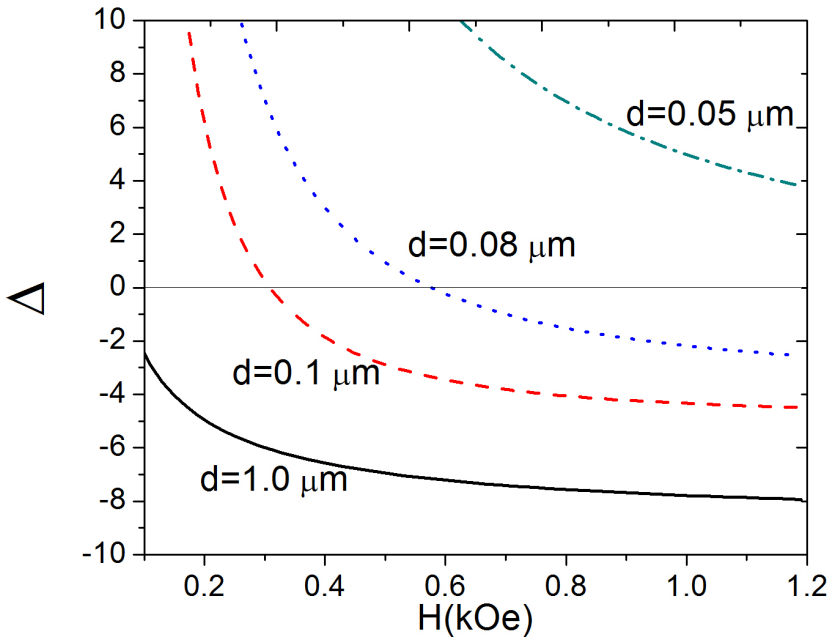

Figure 3.3: The criterion of transition from non-symmetric to symmetric phase, Δ (in units of mK/N), as a function of magnetic field H for different values of thickness d.

phase with $N_Q \neq N_{-Q}$. The transition from symmetric to non-symmetric phase at $\Delta = 0$ is of the second order. There is no metastable state of these phases. At $C = 0$ one finds $\delta = \pm N_c$, which corresponds to a completely non-symmetric phase with only one condensate. The ground state of non-symmetric phase is double-degenerate corresponding to the two possible signs of δ. Fig.3.3 shows that for a film thickness of about 0.05 μm, the symmetric phase is energy favorable up to $H = 1.2$ T. For $d = 0.08$ μm, on increasing H to about 0.6 kOe, there is a transition from symmetric to non-symmetric phase. For a larger thickness $d = 0.1$ μm or $d = 1$ μm, the ground state is non-symmetric for $H > 0.3$ kOe.

3.5 Phase diagram

Fig.3.4 shows that the phase diagram in (d, H) space has three different regions, separated by two critical transition lines, $d_c(H)$ and $d^*(H)$, corresponding to $\Delta = 0$ and $C = 0$, respectively. As shown below, measurement of the contrast, or modulation depth [66], of the spatial interference pattern permits identification of the different condensate phases.

3.6 Comparison with experiment

The ground state wave function $\Psi(z)$ generally is a superposition of two condensate amplitudes

$$\Psi(z) = (c_Q e^{iQz} + c_{-Q} e^{-iQz})/\sqrt{V} \tag{3.21}$$

where

$$c_{\pm Q} = \sqrt{N_{\pm Q}} e^{i\phi_\pm} \tag{3.22}$$

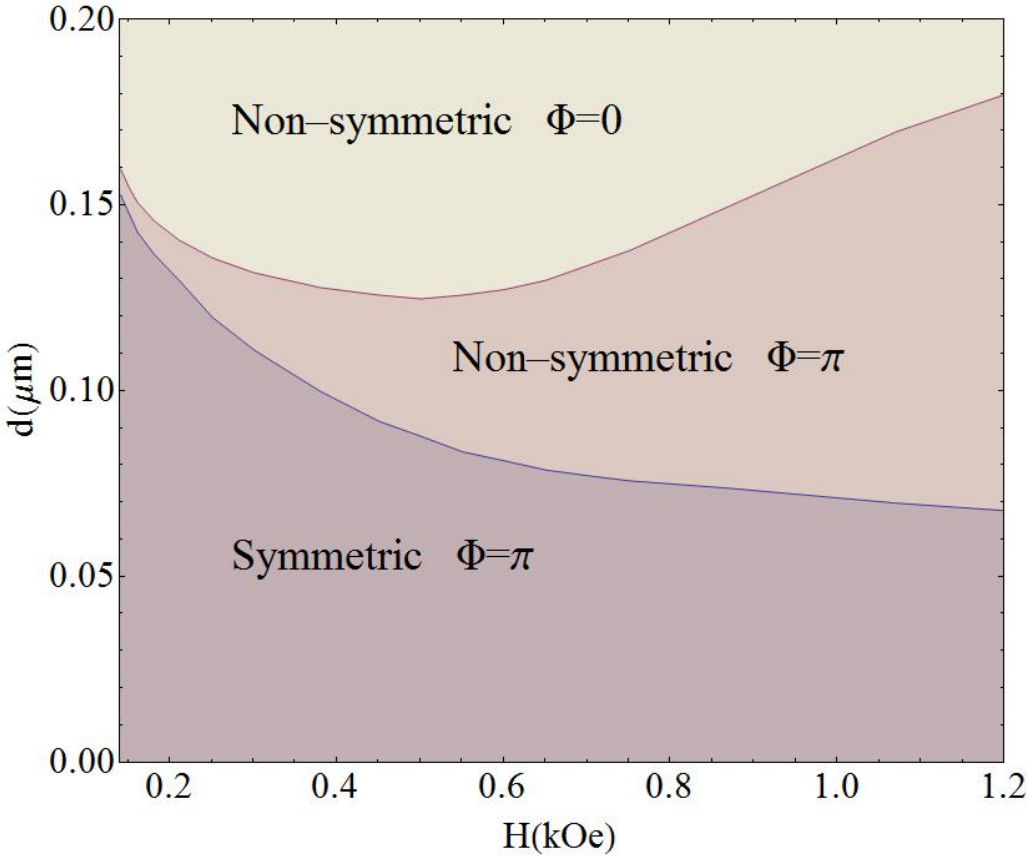

Figure 3.4: The phase diagram for different values of thickness d and magnetic field H.

and V is the volume of the film. The spatial structure of $\Psi(z)$ can be measured by Brillouin Light Scattering (BLS). The BLS intensity is proportional to the condensate density

$$|\Psi|^2 = n_Q + n_{-Q} + 2\sqrt{n_Q n_{-Q}}\cos(2Qz + \phi_+ - \phi_-). \tag{3.23}$$

In their recent experiment, Nowik-Boltyk *el al* [66] observed the interference pattern associated with the ground state. They found that the contrast of this periodic spatial modulation is far below 100%, of the order 3%. The present theory can quantitatively explain this result. In the experiment of Ref.[66], $d = 5.1$ μm and $H = 1$ kOe, eq.(3.17) for A, B and C then gives $A = -0.168$ mK/N, $B = 8.218$ mK/N and $C = -0.203$ mK/N, so $\Delta < 0$. This corresponds to the non-symmetric phase, where the ratio of the numbers of magnons in the two condensates is

$$\frac{N_{-Q}}{N_Q} \approx \frac{C^2}{4(B-A)^2} \tag{3.24}$$

(assume $\delta > 0$). The contrast is defined as

$$\beta = \frac{|\Psi|^2_{max} - |\Psi|^2_{min}}{|\Psi|^2_{max} + |\Psi|^2_{min}}. \tag{3.25}$$

Since $C \ll B$ and $N_{-Q} \ll N_Q$,

$$\beta \approx 2\sqrt{\frac{N_{-Q}}{N_Q}} \approx \frac{|C|}{|B-A|} \tag{3.26}$$

For the above values of A, B and C, β is of order 2.4%, in good agreement with experiment. The smallness of C (and A) in comparison to B is associated with a

large parameter d/l where

$$l = \sqrt{\frac{D}{\pi\gamma M}} \tag{3.27}$$

is an intrinsic length scale of the system and $l \sim 10^{-6}$ m. In terms of this parameter,

$$\frac{|C|}{B} \sim (\frac{l}{d})^{2/3}. \tag{3.28}$$

In the experiment [66] the contrast β reaches the saturation value at comparatively small pumping power corresponding to the appearance of BEC. This agrees with our expression for β, which depends only on film thickness d and magnetic field H. By varying d and H, the contrast can be changed. Specifically, in the symmetric phase, $\beta = 1$; in the non-symmetric phase, $\beta < 1$ and in the completely non-symmetric case with only one condensate, $\beta = 0$. Therefore, measurement of the contrast for different values of d and H can give complete information on the phase diagram of the system, for comparison with the present theory.

Fig.3.5 plots C, Δ and β as functions of the film thickness d at fixed magnetic field $H = 1$ kOe. For small d the system is in the high-contrast symmetric state. At a larger thickness $d_c = 0.07$ μm, the sign of Δ changes, indicating a transition from the symmetric to the low-contrast non-symmetric phase. As d further increases, to $d^* = 0.17$ μm, C changes sign, where the total phase Φ changes from π to 0. Only at this point d^* does the zero-contrast phase with only one condensate appear. Correspondingly, a characteristic cusp in the contrast β appears near d^*.

To conclude, we have calculated the 4-th order magnon-magnon interactions in the condensate, includ- ing magnon-non-conserving term responsible for the coherence of two condensates. We predict a phase transition from symmetric to non-

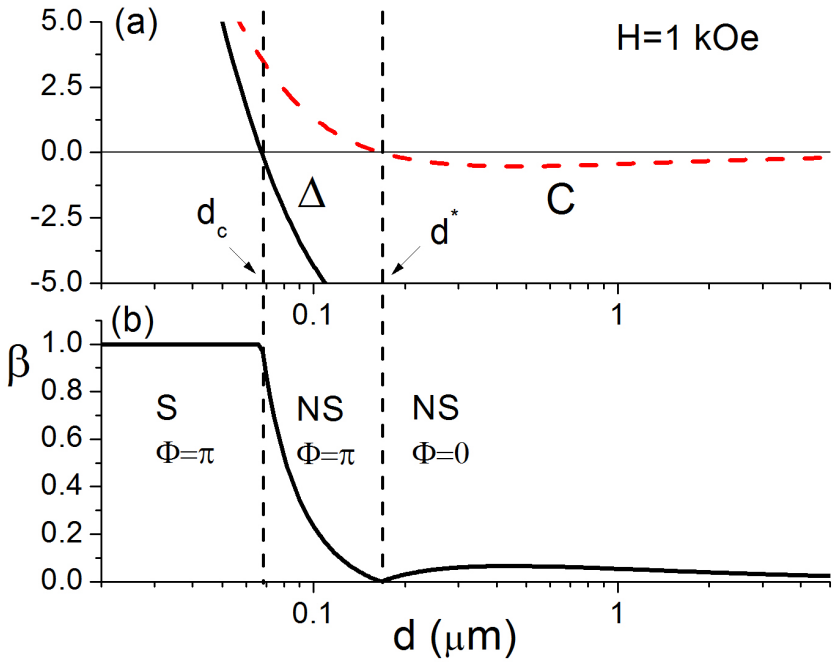

Figure 3.5: (a) Criterion for phase transition Δ and interaction coefficient C as a function of thickness d for fixed magnetic field $H = 1$ kOe. (b) The contrast $\beta = \frac{|\Psi|^2_{max} - |\Psi|^2_{min}}{|\Psi|^2_{max} + |\Psi|^2_{min}}$ as a function of thickness d for $H = 1$ kOe. S and NS denote symmetric and non-symmetric phase, respectively.

symmetric phase that happens at a reasonable magnetic field > 0.2 kOe in sufficiently thin YIG films $d < 0.1$ μm. We also predict that within the non-symmetric phase there is a thickness $d^*(H)$ where the modulation in the observed interference pattern should totally disappear.

3.7 Generalized Gross-Pitaevskii equation

Here we write down the generalized Gross-Pitaevskii equation, and use it to calculate the zero sound spectrum. Let us consider small deviations from the static symmetric solution $n_Q = n_{-Q} = n_c/2$, $\phi_+ = \pi - \phi_- = 0$ so that $n_{\pm Q} = n_c/2 + \delta n_\pm$ with $\delta n_+ = -\delta n_- = \delta n/2$ and $\delta\phi_+ = -\delta\phi_- = \delta\phi/2$.

$$\begin{aligned} E \quad &= \int dr\Big(\frac{\hbar^2}{2m}(|\nabla\Psi_+|^2 + |\nabla\Psi_-|^2) + AV(|\Psi_+|^4 + |\Psi_-|^4) \\ &\quad +2BV|\Psi_+|^2|\Psi_-|^2 + CV(\Psi_+\Psi_- + \Psi_+^*\Psi_-^*)(|\Psi_+|^2 + |\Psi_-|^2)\Big), \end{aligned}$$

On linearizing, the energy reads:

$$E \quad = \int dr\Big(\frac{\hbar^2}{4mn_c}|\nabla\delta n|^2 + \frac{\hbar^2 n_c}{4m}|\nabla\delta\phi|^2 + \frac{\Delta V}{2}\delta n^2\Big). \tag{3.29}$$

Using the commutation relation $[\delta\phi, \delta n] = i$, and the equation of motion $i\hbar\dot{\delta\phi} = [\delta\phi, H]$, we obtain:

$$\hbar\frac{\partial\delta\phi}{\partial t} \quad = -\frac{\hbar^2}{2mn_c}\nabla^2\delta n + \Delta V\delta n, \tag{3.30}$$

$$\hbar\frac{\partial\delta n}{\partial t} \quad = \frac{\hbar^2}{2m}n_c\nabla^2\delta\phi. \tag{3.31}$$

Taking Fourier transforms of the above two equations in coordinate and time, one arrives at dispersion relations Eq.(3.32).

3.8 Zero sound

In two-condensate states the relative phase $\delta\phi = \phi_+ - \phi_-$ is a Goldstone mode. Its oscillation, coupled with the oscillation of the number density $\delta n = n_Q - n_{-Q}$ represents a new branch of collective excitations, which we call zero sound (as in Landau's Fermi liquid, this mode is driven by the self-consistent field rather than collisions). Solving a properly modified Gross-Pitaevskii equation (see Methods), we can find its spectrum. In the symmetric phase it is:

$$\omega = \sqrt{\frac{\hbar^2 k^4}{4m^2} + N_c \Delta \frac{k^2}{m}}. \tag{3.32}$$

The effective mass of magnon is of the order of the electron mass. The density of condensed magnons $n_c = N_c/V$ is about 10^{18} cm^{-3} and $\Delta \approx 10$ mK/N. The sound speed for small k in this case is $v_{0s} = \sqrt{N_c \Delta / m}$, which is about 100 m/s. Near the transition point $\Delta = 0$, the velocity of this zero sound goes to zero. For the non-symmetric case, the spectrum is:

$$\omega = \sqrt{\frac{\hbar^2 k^4}{4m^2}\kappa + N_c (B - A)(\kappa - 1)\frac{k^2}{m}}, \tag{3.33}$$

where $\kappa \equiv \frac{(B-A)^2}{C^2}$. In the experiment [66], $\kappa \sim 10^4$ and $B - A = 8.4$ mK/N. An estimate of the sound speed gives 3×10^3 m/s. The dispersions of zero sound for symmetric and non-symmetric cases are shown in Fig.3.6. Note that the range of applicability of linear approximation strongly shrinks at small C since the density of one of condensates becomes small and the fluctuations of the phase grow.

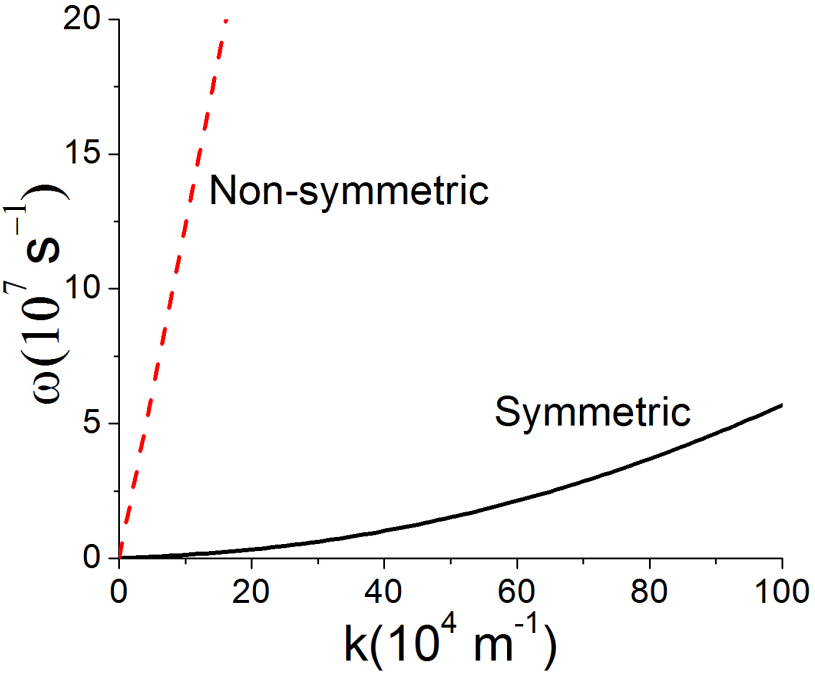

Figure 3.6: Dispersions of zero sound for symmetric and non-symmetric cases, respectively. For the non-symmetric case, we choose $H = 1$ kOe and $d = 5$ μm.

3.9 Domain wall

Since the ground state of the non-symmetric phase is doubly degenerate, it may consist of domains with different signs of δ separated by domain walls. The width w of a domain wall is of the order of $\sqrt{\frac{\hbar^2}{2mN_c|\Delta|}}$. For the data of experiment [66], $w \approx 10$ μm. The energy of domain wall per unit area is $\approx 10^{-9}\mathrm{J/m}^2$.

4. RELAXATION OF CONDENSED MAGNONS DUE TO THREE MAGNON PROCESSES IN FERROMAGNETIC FILM WITH FINITE THICKNESS

4.1 Introduction and motivation

The study of relaxation of magnons in ferromagnetic material, such as yttrium iron garnet, is a long story and can be dated back to 1950s. In the early days, two aspects of relaxation are discussed. First, people were interested in the energy transfer between the whole magnon system and the phonon system [77]. Therefore, in this context, the relaxation time means the time needed for the establishment of equilibrium between the spin and lattice systems. Secondly, due to the experimental development of ferromagnetic spin resonance absorption [83], the uniform mode, that is, the magnons near $\mathbf{k} = 0$ are paid much attention. The line width of ferromagnetic spin resonance was found to be $50-500$ oesterds, corresponding to over-all relaxation time of the order of 10^{-8} to 10^{-9} sec for the uniform mode. The relaxation of this uniform mode are explained through different mechnisms, e.g. the scattering of $k = 0$ modes into degenerate modes by polishing imperfections on the sample surfaces, [82], the four magnon processes originated from exchange interaction [68], three magnons processes due to dipolar interaction [81] and magnon phonon interaction [34, 45, 44, 77, 73].

The discovery of magnon BEC in YIG film arouses the new interest in the study of dynamics and relaxation of magnons due to different mechanisms. The whole picture of magnon BEC can be described as follows: through parallel pumping, additional magnons are pumped to a relatively high energy level. These primary magnons interact with each through four-magnon processes which conserves both the number and energy of magnons, and after a thermalization time of 10 to 100

ns, the system reaches a quasi equilibrium. After that time, the condensed magnons will relax through two different mechanism, magnon-phonon processes and three-magnon processes. Through magnon-phonon processes, the energy of magnon system are transferred to the lattice and disappear. Through three-magnon processes, one condensed magnon with a magnon in the exchange regime merge into one magnon with higher energy; then the latter interacts with the phonon and transfer the energy into lattice.

In a recent work [73], Ruckriegel *et al*, starting from the microscopic Hamiltonian, calculated the phonon contribution to the damping of magnons in the full range of spectrum. Different effects on damping of magnons in different regimes of momentum space are found: in the large wave vector regime, that is, the exchange regime, the magnon damping is dominated by Cherenkov type scattering processes, while in the long-wavelength dipolar regime, these processes are subdominant and the magnon damping is two orders of magnitude smaller. This work shows that in the context of magnon BEC, the mechanism of the relaxation time, or the life time of condensed magnons (in the dipolar regime), is not, or more strictly speaking, is not only due to magnon-phonon processes. In other words, three magnon processes may play a more important role in the relaxation of condensed magnons. Note that four magnon processes conserve the number of magnons, therefore it determines the thermalization time of magnon system but plays a less important role in relaxation.

Our goal in this section is to study the relaxation of condensed magnons due to three magnons processes in a film with finite thickness. The three magnon processes have been studied extensively in experiments [67, 60, 50]. However, there are few theoretical studies on this topic [12, 56]. Our work takes into account higher bands due to the finite thickness of ferromagnetic film and gives the relaxation time of condensed magnons. Our study will deepen our understanding in three magnon process

and would be helpful in developing spin-current based electronics [50].

4.2 Magnons in quasi-2D film.

We start from the following effective quantum spin Hamiltonian which is generally used to describe the magnetic properties of YIG at room temperature:

$$H = -J \sum_{\langle ij \rangle} \mathbf{S}_i \cdot \mathbf{S}_j - g\mu_B H_0 \sum_i S_i^z + H_D \tag{4.1}$$

where the three terms are respectively exchange interaction, Zeeman interaction and dipole interaction. Here we adopt the same geometry as shown in Fig. 2.3. H_0 is the magnitude of external magnetic field along z. $S_i \equiv S(R_i)$ is the spin operator localized at the sites R_i of a cubic lattice with lattice constant $a \approx 12$ $\mathring{A}$. For the exchange interaction, we consider only the nearest neighbor coupling with coupling constant J.

By introducing $\mathbf{S}(\mathbf{r}) = \mathbf{S}_i$, we can change $\sum_i \to \int d\mathbf{r}/a^3$. For finite thickness, we introduce eigenfunctions:

$$\varphi_n = \sqrt{\frac{2}{d}} \sin k_n y \tag{4.2}$$

with

$$k_n = \frac{n\pi}{d} \tag{4.3}$$

when y ranges from 0 to d.

We take the following Fourier transformations:

$$\mathbf{S}(\mathbf{r}) = \sqrt{\frac{2}{N}} \sum_{\mathbf{k}} \sum_{n} e^{i\mathbf{k}\mathbf{r}_{\parallel}} \sin k_n y \mathbf{S}(\mathbf{k}, n) \tag{4.4}$$

or

$$\mathbf{S}_i = \sqrt{\frac{2}{N}} \sum_{\mathbf{k},n} e^{i\mathbf{k}\mathbf{r}_{\parallel}} \sin k_n y \mathbf{S}(\mathbf{k}, n) \tag{4.5}$$

The corresponding inverse Fourier transformation:

$$\mathbf{S}(\mathbf{k}, n) = \sqrt{\frac{2}{N}} \int \frac{d\mathbf{r}}{a^3} e^{-i\mathbf{k}\mathbf{r}_{\parallel}} \sin k_n y \mathbf{S}(\mathbf{r}) \tag{4.6}$$

where

$$\int d\mathbf{r} e^{i\mathbf{k}\mathbf{r}_{\parallel}} \sin k_n y = \frac{V}{2} \delta_{\mathbf{k},0} \delta_{n,0} \tag{4.7}$$

is used. Here, $\mathbf{k}$ is the in plane wave vector and is discritezed. $\int d\mathbf{r}_{\parallel} e^{i(\mathbf{k}-\mathbf{k}')\mathbf{r}_{\parallel}} = A\delta_{\mathbf{k},\mathbf{k}'}$. (Compared with infinite area, which leads to continuous $\mathbf{k}$, $\int d\mathbf{r}_{\parallel} e^{i(\mathbf{k}-\mathbf{k}')\mathbf{r}_{\parallel}} = (2\pi)^2 \delta(\mathbf{k}-\mathbf{k}')$.)

The Zeeman and exchange terms give:

$$H_{ex} + H_Z = -J \sum_{<ij>} (\frac{1}{2} S_i^+ S_j^- + \frac{1}{2} S_i^- S_j^+ + S_i^z S_j^z) - g\mu_B H_0 \sum_i S_i^z \tag{4.8}$$

Up to quadratic orders of $a_{\mathbf{k},n}^{\dagger}$ and $a_{\mathbf{k},n}$, after the Holstein-Primakoff transformation:

$$H_{ex} + J_Z = \sum_{\mathbf{k},n} [D(k^2 + k_n^2) + \hbar\gamma H_0] a_{\mathbf{k},n}^{\dagger} a_{\mathbf{k},n} \tag{4.9}$$

with $D = 2JSa^2$. The contribution to summation due to boundary is neglected.

For dipolar interaction

$$H_D = -\frac{1}{2}(g\mu_B)^2 \sum_{i,j} \frac{(\mathbf{S}_i \mathbf{r}_{ij})(\mathbf{S}_j \mathbf{r}_{ij})}{r_{ij}^5} - \frac{3\mathbf{S}_i \mathbf{S}_j}{r_{ij}^3} \tag{4.10}$$

we first change the summation over lattice into continuous integral over space:

$$H_D = -\frac{1}{2}(g\mu_B)^2 \int \frac{d\mathbf{r}_1 d\mathbf{r}_2}{a^6} \frac{(\mathbf{S}_1 \mathbf{r}_{12})(\mathbf{S}_2 \mathbf{r}_{12})}{r_{12}^5} - \frac{3\mathbf{S}_1 \mathbf{S}_2}{r_{12}^3} \tag{4.11}$$

Then we can rewrite it as:

$$H_D = \frac{1}{2}(g\mu_B)^2 \int \frac{d\mathbf{r}_1 d\mathbf{r}_2}{a^6} (\mathbf{S}_1 \nabla_1)(\mathbf{S}_2 \nabla_2) \frac{1}{r_{12}} \tag{4.12}$$

or

$$H_D = \frac{1}{2}(g\mu_B)^2 \int \frac{d\mathbf{r}_1 d\mathbf{r}_2}{a^6} (\nabla_1 \mathbf{S}_1)(\nabla_2 \mathbf{S}_2) \frac{1}{r_{12}} \tag{4.13}$$

For the boundary condition that we adopt, the surface charge is zero. The above dipolar interaction contains different terms, such as H_D^{xx}, H_D^{yy} and H_D^{zz}. Take H_D^{xx} for example:

$$H_D^{xx} = \frac{1}{2}(g\mu_B)^2 \int \frac{d\mathbf{r}_1 d\mathbf{r}_2}{a^6} S^x(\mathbf{r}_1) S^x(\mathbf{r}_2) \partial_{1,x} \partial_{2,x} \frac{1}{r_{12}} \tag{4.14}$$

Using the Holstein-Primakoff transformation and the following identity:

$$\frac{1}{\sqrt{r_\parallel^2 + y^2}} = \frac{2\pi}{A} \sum_{\mathbf{k}} e^{i\mathbf{k}\mathbf{r}_\parallel} \frac{e^{-k|y|}}{k} \tag{4.15}$$

we have:

$$H_D^{xx} = \frac{1}{2}(g\mu_B)^2 \frac{2S}{4} \int \frac{d\mathbf{r}_1 d\mathbf{r}_2}{a^6} (a_1^\dagger + a_1)(a_2^\dagger + a_2) \frac{2\pi}{A} \sum_{\mathbf{k}} \frac{k_x^2}{k} e^{-k|y_1 - y_2|} e^{i\mathbf{k}(\mathbf{r}_{\parallel,1} - \mathbf{r}_{\parallel,2})} \quad (4.16)$$

and then make the Fourier transformation of $a_1 \equiv a_{\mathbf{r}_1}$ and a_2, and perform the integral over $\mathbf{r}_1$ and $\mathbf{r}_2$

$$H_D^{xx} = (g\mu_B)^2 \frac{4\pi S}{4a^3} \sum_{\mathbf{k}} \sum_{n,n'} \frac{k_x^2}{k^2} F_{nn'}(kd)[(a_{\mathbf{k},n}^\dagger + a_{-\mathbf{k},n})(a_{-\mathbf{k},n'}^\dagger + a_{\mathbf{k},n'})] \quad (4.17)$$

We introduce the magnetization in terms of the effective spin and lattice constant a:

$$M = g\mu_B \frac{S}{a^3} \quad (4.18)$$

therefore,

$$\begin{aligned} H_D^{xx} \quad &= \hbar\gamma 4\pi M \sum_{\mathbf{k}} \sum_{n,n'} \frac{k_x^2}{k^2} \frac{F_{nn'}}{2} a_{\mathbf{k},n}^\dagger a_{\mathbf{k},n'} \\ &+ \hbar\gamma 4\pi M \sum_{\mathbf{k}} \sum_{n,n'} \frac{k_x^2}{k^2} \frac{F_{nn'}}{4} (a_{\mathbf{k},n}^\dagger a_{-\mathbf{k},n'}^\dagger + a_{-\mathbf{k},n} a_{\mathbf{k},n'}) \end{aligned} \quad (4.19)$$

The dimensionless form factor:

$$\begin{aligned} F_{nn'} \quad &= \frac{k}{d} \int_0^d dy_1 dy_2 e^{-k|y_1 - y_2|} \sin k_1 y_1 \sin k_2 y_2 \\ &= \frac{k}{d} \frac{kd}{k^2 + k_1^2} \delta_{n,n'} + \frac{k}{d} \frac{k_1 k_2}{(k^2 + k_1^2)(k^2 + k_2^2)} \Big[1 + (-1)^{n+n'} \\ &\qquad - e^{-kd}(-1)^{n'} - e^{-kd}(-1)^n \Big] \end{aligned} \quad (4.20)$$

Similarly

$$H_D^{yy} = \hbar\gamma 4\pi M \sum_{\mathbf{k}} \sum_{n,n'} \frac{G_{nn'}}{2} a^\dagger_{\mathbf{k},n} a_{\mathbf{k},n'} \tag{4.21}$$

$$-\hbar\gamma 4\pi M \sum_{\mathbf{k}} \sum_{n,n'} \frac{G_{nn'}}{4} (a^\dagger_{\mathbf{k},n} a^\dagger_{-\mathbf{k},n'} + a_{-\mathbf{k},n} a_{\mathbf{k},n'}) \tag{4.22}$$

in which

$$\begin{aligned} G_{nn'} &= \frac{k_1 k_2}{kd} \int_0^d dy_1 dy_2 e^{-k|y_1 - y_2|} \cos k_1 y_1 \cos k_2 y_2 \\ &= \frac{k_1 k_2}{kd} \frac{kd}{k^2 + k_1^2} \delta_{n,n'} - \frac{k_1 k_2}{kd} \frac{k^2}{(k^2 + k_1^2)(k^2 + k_2^2)} [1 + (-1)^{n+n'} \\ &\qquad - e^{-kd}(-1)^{n'} - e^{-kd}(-1)^n] \end{aligned} \tag{4.23}$$

Here k_1 and k_2 should be understood as k_{n_1} and k_{n_2}, respectively.

Here we list some Useful expressions:

$$\int_0^y \sin k_1 y e^{ky} dy = \frac{k e^{ky} \sin k_1 y - k_1 e^{ky} \cos k_1 y + k_1}{k^2 + k_1^2} \tag{4.24}$$

$$\int_0^y \cos k_1 y e^{ky} dy = \frac{k e^{ky} \cos k_1 y + k_1 e^{ky} \sin k_1 y - k}{k^2 + k_1^2} \tag{4.25}$$

$$\int_0^d \sin k_1 y e^{ky} dy = \frac{-k_1 e^{kd}(-1)^n + k_1}{k^2 + k_1^2} \tag{4.26}$$

$$\int_0^d \cos k_1 y e^{ky} dy = \frac{k e^{kd}(-1)^n - k}{k^2 + k_1^2} \tag{4.27}$$

$$\int_0^d \sin k_1 y \sin k_2 y = \frac{d}{2} \delta_{n,n'} \tag{4.28}$$

$$\int_0^d \sin k_1 y \cos k_2 y = k_1 \frac{1 - (-1)^{n+n'}}{k_1^2 - k_2^2} \tag{4.29}$$

$$\int_0^d \cos k_1 y \cos k_2 y \qquad = \frac{d}{2}\delta_{n,n'} \tag{4.30}$$

4.3 Magnon spectrum in quasi-2D: diagonal approximation

Generally, the Hamiltonian, up to the quadratic order of $a^\dagger_{n,\mathbf{k}}$ and $a_{n,\mathbf{k}}$, can be written as:

$$H = \sum_{\mathbf{k},n,n'} A_{nn'} a^\dagger_{n,\mathbf{k}} a_{n',\mathbf{k}} + \frac{B_{n,n'}}{2}[a^\dagger_{n,k} a^\dagger_{n',-k} + a_{n,k} a_{n',-k}] \tag{4.31}$$

with

$$A_{nn'} \quad = [\hbar\gamma H_0 + D(k^2 + k_n^2)]\delta_{n,n'} + 2\pi\hbar\gamma M \sin^2\theta_k F_{nn'} + 2\pi\hbar\gamma M G_{nn'} \tag{4.32}$$

$$B_{nn'} \quad = 2\pi\hbar\gamma M \sin^2\theta_k F_{nn'} - 2\pi\hbar\gamma M G_{nn'} \tag{4.33}$$

where $F_{nn'}$ and $G_{nn'}$ have been given in Eq. 4.20 and Eq. 4.23.

If we consider only the diagonal matrix elements, and treat the $n \neq n'$ terms as perturbation, then we can have a first order approximation

$$H_0 = \sum_{\mathbf{k},n} A_n a^\dagger_{n,\mathbf{k}} a_{n,\mathbf{k}} + \frac{B_n}{2}[a^\dagger_{n,k} a^\dagger_{n,-k} + a_{n,k} a_{n,-k}] \tag{4.34}$$

with

$$A_n \quad = [\hbar\gamma H_0 + D(k^2 + k_n^2)] + 2\pi\hbar\gamma M \sin^2\theta_k F_{nn} + 2\pi\hbar\gamma M G_{nn} \tag{4.35}$$

$$B_n \quad = 2\pi\hbar\gamma M \sin^2\theta_k F_{nn} - 2\pi\hbar\gamma M G_{nn} \tag{4.36}$$

and

$$F_{nn} = \frac{k^2}{k^2+k_n^2} + 2\frac{k}{d}\frac{k_n^2}{(k^2+k_n^2)^2}[1-e^{-kd}] \tag{4.37}$$

$$G_{nn} = \frac{k_n^2}{k^2+k_n^2} - 2\frac{k}{d}\frac{k_n^2}{(k^2+k_n^2)^2}[1-e^{-kd}] \tag{4.38}$$

and we notice that

$$F_{nn} = 1 - G_{nn} \tag{4.39}$$

The spectrum can be readily obtained:

$$\omega_n = \sqrt{(\epsilon_n + mG_{nn})(\epsilon_n + m\sin^2\theta(1-G_{nn}))} \tag{4.40}$$

where $m \equiv 4\pi\hbar\gamma M$ and $\epsilon_n = \hbar\gamma H_0 + D(k^2+k_n^2)$.

Here,we used the Bogoliubov transformation:

$$a_{n,\mathbf{k}} = u_{n,\mathbf{k}}c_{n,\mathbf{k}} + v_{n,\mathbf{k}}c^\dagger_{n,-\mathbf{k}} \tag{4.41}$$

with

$$u_{n,\mathbf{k}} = u_{n,-\mathbf{k}} = (\frac{A_{n,\mathbf{k}}+\omega_{n,\mathbf{k}}}{\omega_{n,\mathbf{k}}})^{1/2} \tag{4.42}$$

$$v_{n,\mathbf{k}} = -sign(B_{n,\mathbf{k}})(\frac{A_{n,\mathbf{k}}-\omega_{n,\mathbf{k}}}{\omega_{n,\mathbf{k}}})^{1/2} \tag{4.43}$$

Notice that in the vicinity of $k = 0$, the above expression is the exact answer, because the non diagonal matrix elements vanish as $k = 0$. Therefore at least in this limit $k \sim 0$, this approximation is good. In Fig. 4.1 and Fig. 4.2 we plot the magnon

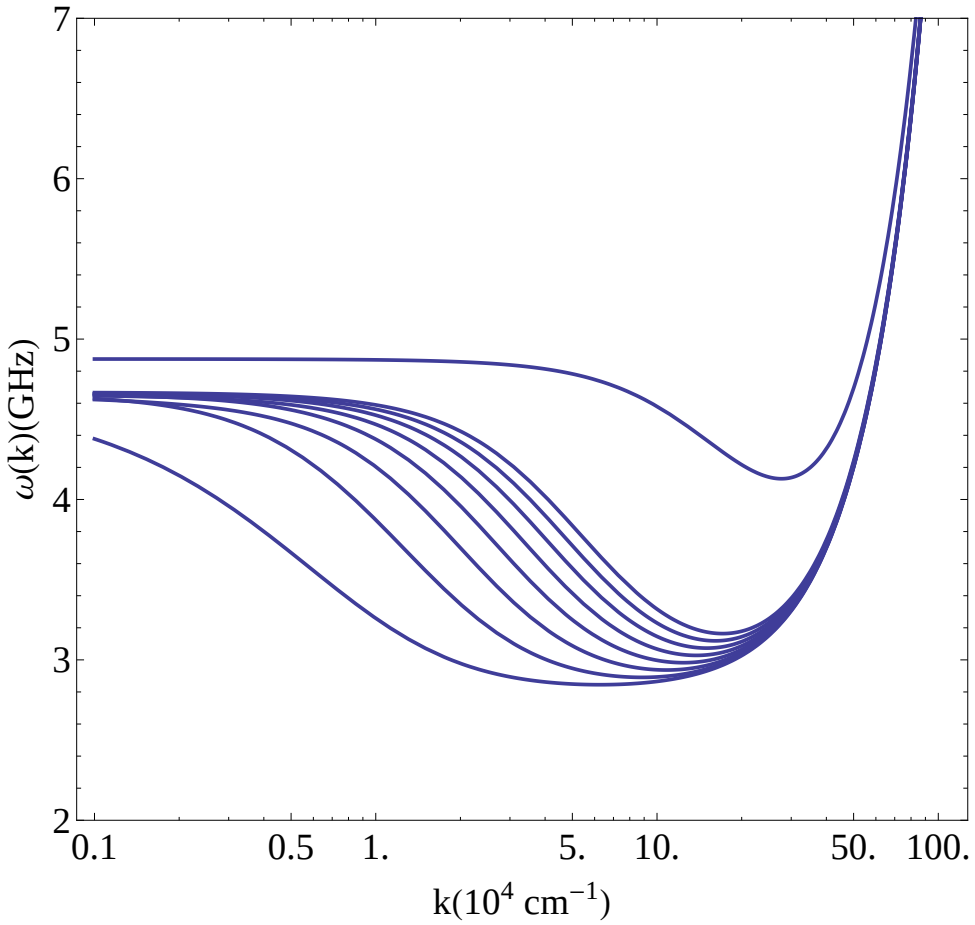

Figure 4.1: Magnon spectrum in quasi-2D film with finite thickness. From below to above, the curves correspond to $n = 1, 2, 3, 4, 5, 6, 7, 8, 30$, respectively. $d = 5$ μm, $H_0 = 1.0$ kOe

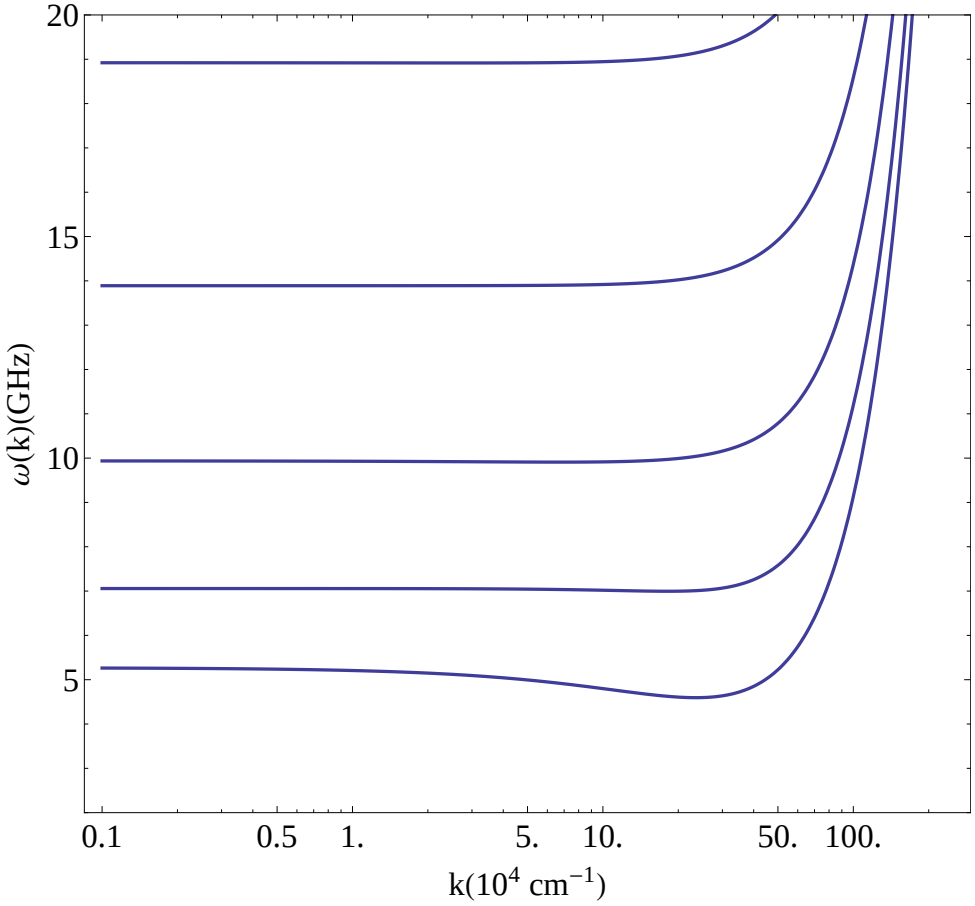

Figure 4.2: Magnon spectrum in quasi-2D film with finite thickness. From below to above, the curves correspond to $n = 1, 2, 3, 4, 5$, respectively. $d = 0.1$ μm, $H_0 = 1.0$ kOe

spectrum given by Eq. 4.40 with $d = 5\mu$m and $d = 0.1$ μm, respectively. Similar results are also obtained in Ref. [48] and [32, 15],

4.3.1 Lowest level

For lowest level, we would have:

$$H_0 = \hbar \sum_{\mathbf{k}} A_k a_k^\dagger a_k + \frac{1}{2} B_k a_k a_{-k} + \frac{1}{2} B_k^* a_k^\dagger a_{-k}^\dagger, \tag{4.44}$$

with

$$A_k = \quad [\gamma H_0 + D(k^2 + (\pi/d)^2) + \gamma 2\pi M F_{11} \sin^2\theta + \gamma 2\pi M G_{11}] \tag{4.45}$$

$$B_k = \quad [\gamma 2\pi M F_{11} \sin^2\theta - \gamma 2\pi M G_{11}] \tag{4.46}$$

in which

$$F_{11} = 1 - G_{11} = \frac{x^2}{x^2 + \pi^2} + \frac{x\pi^2}{(x^2 + \pi^2)^2} 2(1 + e^{-x}) \tag{4.47}$$

In this approximation, we find that the nonzero wavevector Q at the minimum energy point is $Q = 6.25 \times 10^4$ cm^{-1}, when we take $D/\gamma = 2 \times 10^{-9}$ Oe cm ^{2} and $d = 5\mu$m, $H_0 = 1$ kOe. This Q is smaller than the value in the uniform approximation $Q = 7.55 \times 10^4$ cm^{-1} obtained from Eq. 2.77.

4.4 3-magnon process

3-magnon interaction comes from two parts in the dipolar interaction: H_D^{xz} and H_D^{yz}:

$$H_D^{xz} = 2\frac{(g\mu_B)^2}{2} \int \frac{d\mathbf{r}_1 d\mathbf{r}_2}{a^6} S_1^x S_2^z \partial_{1x} \partial_{2z} \frac{1}{r_{12}} \tag{4.48}$$

factor 2 is due to the $S_1^z S_2^x$ term which gives the identical contribution with $S_1^x S_2^z$ term.

$$H_D^{xz} = (g\mu_B)^2 \int \frac{d\mathbf{r}_1 d\mathbf{r}_2}{a^6} \frac{\sqrt{2S}}{2} (a_1^\dagger + a_1)(-a_2^\dagger a_2) \partial_{1x} \partial_{2z} \frac{1}{r_{12}} \tag{4.49}$$

Making a Fourier transformation and integrating over space coordinates, we have:

$$H_D^{xz} = -\frac{\hbar\gamma 4\pi M}{\sqrt{SN}} \sum_{\mathbf{k},\mathbf{q}} \sum_{n_1 n_2 n_3} A^{(3)}(\mathbf{k}, \mathbf{q}, n_1, n_2, n_3)(a_{kn_1}^\dagger a_{qn_2}^\dagger a_{k+q,n_3} + a_{k+q,n_3}^\dagger a_{qn_2} a_{kn_1}) \tag{4.50}$$

The coefficient is:

$$A^{(3)}(\mathbf{k}, \mathbf{q}, n_1, n_2, n_3) = \frac{1}{2}\Big[\frac{k_x k_z}{2k^2}\left[J_{n_1,|n_2-n_3|}(k) - J_{n_1,n_2+n_3}(k)\right] \tag{4.51}$$

$$+ \frac{q_x q_z}{2q^2}\left[J_{n_2,|n_1-n_3|}(q) - J_{n_2,n_1+n_3}(q)\right] \tag{4.52}$$

with

$$J_{n_1,n_2}(k) \quad = \frac{k}{d} I_{sc}(n_1, n_2; k) \tag{4.53}$$

Another contribution from

$$H_D^{yz} = 2\frac{(g\mu_B)^2}{2} \int \frac{d\mathbf{r}_1 d\mathbf{r}_2}{a^6} S_1^y S_2^z \partial_{1y} \partial_{2z} \frac{1}{r_{12}} \tag{4.54}$$

$$H_D^{yz} = \frac{\hbar\gamma 4\pi M}{\sqrt{SN}} \sum_{\mathbf{k},\mathbf{q}} \sum_{n_1 n_2 n_3} B^{(3)}(\mathbf{k}, \mathbf{q}, n_1, n_2, n_3)(a_{kn_1}^\dagger a_{qn_2}^\dagger a_{k+q,n_3} + a_{k+q,n_3}^\dagger a_{qn_2} a_{kn_1}) \tag{4.55}$$

The coefficient is:

$$B^{(3)}(\mathbf{k},\mathbf{q},n_1,n_2,n_3) = \frac{1}{2}\frac{k_z}{2k}\left[J'_{n_1,|n_2-n_3|}(k) - J'_{n_1,n_2+n_3}(k)\right] + \frac{q_z}{2q}\left[J'_{n_2,|n_1-n_3|}(q) - J'_{n_2,n_1+n_3}(q)\right] \tag{4.56}$$

with

$$J'_{n_1,n_2}(k) = \frac{k_{n_1}}{d} I_{cc}(n_1,n_2;k) \tag{4.57}$$

Here we introduce three integrals:

$$\begin{aligned}
I_{ss} &= \int_0^d dy_1 dy_2 e^{-k|y_1-y_2|}\sin k_1 y_1 \sin k_2 y_2 \\
&= \frac{kd}{k^2+k_1^2}\delta_{n,n'} + \frac{k_1 k_2}{(k^2+k_1^2)(k^2+k_2^2)}[1+(-1)^{n+n'} - e^{-kd}(-1)^{n'} - e^{-kd}(-1)^n] \\
I_{sc} &= \int_0^d dy_1 dy_2 e^{-k|y_1-y_2|}\sin k_1 y_1 \cos k_2 y_2 \\
&= \frac{2kk_1}{k^2+k_1^2}\frac{1-(-1)^{n_1+n_2}}{k_1^2-k_2^2} + \frac{kk_1}{(k^2+k_1^2)(k^2+k_2^2)}[-1+(-1)^{n_1+n_2} + e^{-kd}[(-1)^{n_1} - (-1)^{n_2})]] \\
I_{cc} &= \int_0^d dy_1 dy_2 e^{-k|y_1-y_2|}\cos k_1 y_1 \cos k_2 y_2 \\
&= \frac{kd}{k^2+k_1^2}\delta_{n,n'} - \frac{k^2}{(k^2+k_1^2)(k^2+k_2^2)}[1+(-1)^{n+n'} - e^{-kd}(-1)^{n'} - e^{-kd}(-1)^n]
\end{aligned}$$

Note: when $n_1 = n_2$, $I_{sc} = 0$.

Therefore, totally

$$H^{(3)} = \frac{\hbar\gamma 2\pi M}{\sqrt{SN}} \sum_{\mathbf{k}_1,\mathbf{k}_2,\mathbf{k}_3} \sum_{n_1,n_2,n_3} (D_{1;,n_1,n_2,n_3} + D_{2,n_2,n_1,n_3})\delta_{1+2,3}(a^\dagger_{1,n1}a^\dagger_{2,n_2}a_{3,n_3} + h.c.) \tag{4.58}$$

with

$$D_{\mathbf{k};n_1,n_2,n_3} = \frac{k_z}{2k}\left[J'_{n_1,|n_2-n_3|}(k) - J'_{n_1,n_2+n_3}(k)\right] - \frac{k_x k_z}{2k^2}\left[J_{n_1,|n_2-n_3|}(k) - J_{n_1,n_2+n_3}(k)\right] \tag{4.59}$$

The coefficient $D_{\mathbf{k};n_1,n_2,n_3}$ is a function of only one wave vector, and the order of n_1, n_2, n_3 are important. The Hamiltonian is symmetric with respect to the exchange of $(1, n_1)$ and $(2, n_2)$.

4.4.1 Explicit expressions for 3 magnon interaction.

In the three magnon process, a magnon with wave vector k and another one with q scatter into one with $k + q$. If k is neat the minimum, then $k_x = 0$, $k_z = Q$, the wavevector of other magnon will be very large compared to $1/d$: $q \ll k_n$ for not too large n. Let's consider the process $(k, n_1) + (q, n_2) \to ((k + q), n_3)$, with k located near the minimum point Q, and $n_1 = 1$. There are two different cases for n_2 and n_3 that can simplify $D_{q;n_2,n_1,n_3}$

(1) $n_2 - n_3$ is even. In this case, J' will be zero.

$$D_{q;n_2,n_1,n_3} = -\frac{q_x q_z}{2q^2}[J_{n_2,n_1-n_3}(q) - J_{n_2,n_1+n_3}(q)] \tag{4.60}$$

For the condition $q \gg 1/d$,

$$D_{q;n_2,n_1,n_3} = -\frac{q_x q_z}{q^2 + k_{n_2}^2}\frac{2k_{n_2}}{d}[\frac{1}{k_{n_2}^2 - k_{n_1-n_3}^2} - \frac{1}{k_{n_2}^2 - k_{n_1+n_3}^2}] \tag{4.61}$$

$$= -\frac{8q_x q_z}{\pi(q^2 + k_{n_2}^2)}\frac{n_1 n_2 n_3}{[(n_2+n_3)^2 - n_1^2][(n_2-n_3)^2 - n_1^2]} \tag{4.62}$$

Take the special case for an example: $n_1 = n_2 = n_3 = 1$, we have:

$$D_{q;n_2,n_1,n_3} = -\frac{q_x q_z}{q^2 + k_{n_2}^2}\frac{2}{d}[\frac{1}{k_{n_2}} + \frac{1}{k_{n_2+n_1+n_3}}] \tag{4.63}$$

$$\sim -\frac{q_x q_z}{q^2 + k_{n_2}^2}\frac{8\pi}{3} \tag{4.64}$$

For another limit $n_1 = 1$, $n_2 = n_3 \gg 1$,

$$D_{q;n_2,n_1,n_3} = -\frac{q_x q_z}{q^2 + k_{n_2}^2}\pi \tag{4.65}$$

(2) $n_2 - n_3$ is odd. Terms including J will be zero. Because the delta function in J', the main contribution will be the case: $|n_1 - n_3| = n_2$. For example, here we consider $n_1 = 1$, and $n_2 = n_3 \pm 1$. For the case $n_2 = n_3 - n_1$,

$$D_{q;n_2,n_1,n_3} = \frac{q_z k_{n_2}}{2(q^2 + k_{n_2}^2)} \tag{4.66}$$

for $n_2 = n_3 + n_1$,

$$D_{q;n_2,n_1,n_3} = -\frac{q_z k_{n_2}}{2(q^2 + k_{n_2}^2)} \tag{4.67}$$

After the Bogoliubov transformation, the interaction becomes more complicated. In terms of $D_{\mathbf{k};n_1,n_2,n_3}$, we define

$$\begin{aligned}\alpha(1,2;n_1,n_2,n_3) = \quad & D_{1;n_1,n_2,n_3}u_1u_2u_3 + D_{1;,n_1,n_3,n_2}u_1v_2v_3 \\ & + D_{-1;n_1,n_3,n_2}v_1u_2u_3 + D_{-1;n_1,n_2,n_3}v_1v_2v_3 \\ & + D_{-(1+2);n_3,n_2,n_1}v_1u_2v_3 + D_{1+2;n_3,n_2,n_1}u_1v_2u_3\end{aligned} \tag{4.68}$$

And then by symmetrizing the above coefficient by exchange $(1, n_1)$ and $2, n_2$, we

get the interaction coefficient

$$H^{(3)} = \frac{\hbar\gamma 2\pi M}{\sqrt{SN}} \sum_{\mathbf{k}_1,\mathbf{k}_2,\mathbf{k}_3} \sum_{n_1,n_2,n_3} (\alpha(1,2;n_1,n_2,n_3) + \alpha(2,1,n_2,n_1,n_3)) \times \delta_{1+2,3} \left(c^\dagger_{1,n1} c^\dagger_{2,n_2} c_{3,n_3} + h.c. \right) \tag{4.69}$$

with some other terms containing, e.g., *ccc*, which are neglected.

4.5 Decay time due to three magnon processes

The kinetic equation under the 3-magnon processes can be written as follows:

$$\frac{dn_{k,n_1}}{dt} = \sum_{n2,n3} \sum_{q} W(k,q,n_1,n_2,n_3)[n(k+q,n_3)(n(k,n_1)+1)(n(q,n_2)+1) - (n(k+q,n_3)+1)n(k,n_1)n(q,n_2)] \tag{4.70}$$

with

$$W(k,q,n_1,n_2,n_3) = \frac{2\pi}{\hbar} |I^{(3)}(k,q,n_1,n_2,n_3)|^2 \delta(\omega_{k+q}(n_3) - \omega_k(n_1) - \omega_q(n_2)) \tag{4.71}$$

It includes the confluent process in which two magnons combine together to one magnon, and the splitting process in which a high energy magnon spits into two magnons with lower energy.

If only n_{k,n_1} has a small deviation, we can use the relaxation approximation:

$$\frac{1}{\tau_{k,n_1}} = \sum_{q,n_2,n_3} \frac{2\pi}{\hbar} \frac{(\hbar\gamma 4\pi M)^2}{SN} |I^{(3)}(k,q,n_1,n_2,n_3)|^2 \delta(\omega_{k+q}(n_3) - \omega_k(n_1) - \omega_q(n_2))[n(q,n_2) - n(k+q,n_3)] \tag{4.72}$$

Here, $I^{(3)}$ is the interaction strength.

We consider the case of $d = 5$ μm, and $H \sim 1$kOe. In this case, the minimum

point Q follows $Qd \sim 37$. The energy conservation law requires:

$$\omega_{n_1}(k) + \omega_{n_2}(q) = \omega_{n_3}(k+q) \tag{4.73}$$

If we require both $k \ll 1/d$ and $q \ll 1/d$, then we can approximately write the magnon spectrum as:

$$\omega_n(k) = \hbar\gamma H_0 + D(k^2 + k_n^2) \tag{4.74}$$

The above energy condition becomes:

$$(\omega_{n_1,k} - Dk^2) - D(k_{n_3}^2 - k_{n_2}^2) = 2Dkq_z \tag{4.75}$$

In the previous section, we give the explicit expressions for three magnon interaction, $I^{(3)}(k, q, n_1, n_2, n_3)$.

For $n_2 - n_3$ even, we have:

$$\begin{aligned}\frac{1}{\tau_{k,n_1}} = & \sum_{n_2,n_3} \frac{2\pi}{\hbar} \frac{(\hbar\gamma 4\pi M)^2}{S} \frac{a^3}{d} \int \frac{dq_x dq_y}{(2\pi)^2} \frac{64 q_x^2 q_z^2}{\pi^2 (q^2 + k_{n_2}^2)^2} \frac{n_1^2 n_2^2 n_3^2}{[(n_2+n_3)^2 - n_1^2]^2 [(n_2 n_3)^2 - n_1^2]^2} \\ & \frac{T\omega_{n_1}(k)}{\omega(n_2, q)^2} \delta(\omega_{k+q}(n_3) - \omega_k(n_1) - \omega_q(n_2))\end{aligned} \tag{4.76}$$

Integrating over q_z, we can eliminate the delta function, the result is to replace q_z by

$$q0_z \equiv ((\omega_{n_1,k} - Dk^2) - D(k_{n_3}^2 - k_{n_2}^2))/2Dk \tag{4.77}$$

we get:

$$\frac{1}{\tau_{k,n_1}} = \sum_{n_2,n_3} \frac{2\pi}{\hbar} \frac{(\hbar\gamma 4\pi M)^2}{S} \frac{a^3}{d} \int \frac{dq_x}{(2\pi)^2} \frac{64 q_x^2 q0_z^2}{2Dk\pi^2 (q^2 + k_{n_2}^2)^2} \tag{4.78}$$

$$\frac{n_1^2 n_2^2 n_3^2}{[(n_2+n_3)^2-n_1^2]^2[(n_2 n_3)^2-n_1^2]^2}\frac{T\omega_{n_1}(k)}{\omega(n_2,q)^2} \tag{4.79}$$

Then we can make a change of variable from q_x to $x = q_x d$, we define:

$$z = q0_z d = ((\omega_{n_1,k} - Dk^2) - D(k_{n_3}^2 - k_{n_2}^2))d/2Dk \tag{4.80}$$

$$a^2 = z^2 + n_2^2\pi^2 \tag{4.81}$$

$$b^2 = z^2 + n_2^2\pi^2 + \hbar\gamma H_0/(D/d^2)) \tag{4.82}$$

and we used

$$\int dx \frac{x^2}{(x^2+a^2)^2(x^2+b^2)^2} = \frac{\pi}{2ab(a+b)^3} \tag{4.83}$$

then we get:

$$\frac{1}{\tau_{k,n_1}} = \frac{2\pi}{\hbar}\frac{(\hbar\gamma 4\pi M)^2}{4\pi^4 S}\frac{T\omega(n_1,k)(kd)^5}{D^3k^6}\frac{a^3}{d^3}f(D/d^2,\hbar\gamma H_0) \tag{4.84}$$

with

$$f(D/d^2,\hbar\gamma H_0) = \sum_{n_2-n_3 even}\frac{32\pi z^2}{ab(a+b)^3}\frac{n_1^2 n_2^2 n_3^2}{[(n_2+n_3)^2-n_1^2]^2[(n_2-n_3)^2-n_1^2]^2} \tag{4.85}$$

Due to the $[(n_2-n_3)^2-n_1^2]^2$ in the denominator, function f decreases rapidly as one increase $n_2 - n_3$. If we consider Numerical calculation gives:

$$n_2 = n_3, f = 7.3 * 10^{-7}, \tag{4.86}$$

$$n_2 - n_3 = 2, f = 8.6 * 10^{-8}. \tag{4.87}$$

$$n_2 - n_3 = -2, f = 7.1 * 10^{-8} \tag{4.88}$$

$$n_2 - n_3 = 4, f = 3.8 * 10^{-9} \tag{4.89}$$

$$n_2 - n_3 = -4, f = 2.4 * 10^{-9} \tag{4.90}$$

$$n_2 - n_3 = 6, f = 7.2 * 10^{-10} \tag{4.91}$$

$$n_2 - n_3 = 6, f = 7.2 * 10^{-10} \tag{4.92}$$

For comparison with experiments, $d = 6.7$ μm, $H_0 = 1.76$ kOe. For the $T = 300K = 6000GHz$, $kd = 33$, $Dk^2 = \frac{\hbar\gamma 4\pi M}{kd}$,

$$\frac{(\hbar\gamma 4\pi M)^2}{S}\frac{T\omega(n_1,k)(kd)^5}{D^3k^6}\frac{a^3}{d^3} = \frac{(kd)^8 T}{S}\frac{a^3}{d^3} = 5.4 * 10^3 GHz \tag{4.93}$$

,

$$\frac{1}{\tau} = \frac{2\pi 5.4 * 10^3}{4\pi^4} * (7.3 + 0.86 + 0.71) * 10^{-7} GHz = 7.7 * 10^4 Hz \tag{4.94}$$

For $n_2 - n_3$ odd, we have:

$$\frac{1}{\tau_{k,n_1}} = \frac{2\pi}{\hbar}\frac{(\hbar\gamma 4\pi M)^2}{128\pi^2 S}\frac{T\omega(n_1,k)(kd)^5}{D^3k^6}\frac{a^3}{d^3} g(D/d^2, \hbar\gamma H_0) \tag{4.95}$$

with

$$g(D/d^2, \hbar\gamma H_0) = \sum_{n_2}\int dx \frac{z^2(\pi n_2)^2}{(x^2 + z^2 + n_2^2\pi^2)^2(x^2 + z^2 + n_2^2\pi^2 + \hbar\gamma H_0/(D/d^2))^2} \tag{4.96}$$

with $n_3 = n_2 - n_1$ or $n_3 = n_2 + n_1$.

The fist case gives $g = 1.6 * 10^{-7}$ and the latter gives: $g = 1.4 * 10^{-7}$.

To conclude, totally, we have a decay rate

$$\frac{1}{\tau} = 1.07 * 10^5 Hz \tag{4.97}$$

4.6 Comparison with the uniform method

In the uniform approximation as was done in Section 3, the third order term, that is, the three magnon term, is given by $H^{(3)}$:

$$H^{(3)} = \sum_{\mathbf{k},q} (f_0(k) + f_0(q))[a_k^\dagger a_q^\dagger a_{q+k} + a_{q+k}^\dagger a_q a_k] \tag{4.98}$$

with

$$f_0(k) = \frac{\hbar\gamma 4\pi M}{2\sqrt{2SN}}(F_k - 1)\frac{k_x k_z}{k^2} \tag{4.99}$$

Using similar procedure and approximations, we have:

$$\frac{1}{\tau_{k,n_1}} = \frac{2\pi}{\hbar}\frac{(\hbar\gamma 4\pi M)^2}{128\pi S}\frac{T\omega_{k,n_1}}{(\hbar\gamma H_0)^3}\frac{a}{d}(ka)^2 \tag{4.100}$$

Substituting the values of parameters in the case for $d = 5.1\mu$m and $H_0 = 1.0$ kOe, we have:

$$\frac{1}{\tau_Q} \sim 100 Hz \tag{4.101}$$

which is much smaller than the result for a film with finite thickness.

4.7 Comparison with decay due to magnon phonon interaction and conclusion

The treatment of magnon-phonon interaction are either phenomenologically using the magnetoelastic coupling of magnons and phonons[34, 82, 77], or microscopically

starting from the Heisenberg model for the exchange interaction with the exchange coefficient as a function of displacement [69, 33, 73]. For example, in the work of Kittel, he used the phenomenological magnetoelastic energy density

$$f_{me} = b_1 \left(\alpha_x^2 S_{xx} + \alpha_y^2 S_{yy} + \alpha_z^2 S_{zz}\right) + 2b_2(\alpha_x\alpha_y S_{xy} + \alpha_y\alpha_z S_{yz} + \alpha_z\alpha_x S_{xz}) \quad (4.102)$$

in which b_i (i=1,2) are two parameters, S_{ij} is the shear components and $\alpha_{x,y,z}$ are the components of unit magnetization. However, Kittel was interested only in the relaxation of the uniform mode. He found that the magnon-phonon process gives rise to a relaxation time of the order of 10^{-1} to 10^{-2} sec for the $k = 0$ magnon.

In the recent work done by Ruckriegel *et al* [73], the phenomenological description of magnetoelastic Hamiltonian is used:

$$H_{me} = H_{ms} + H_{ex} \quad (4.103)$$

with

$$H_{ms} = \gamma' \int M_i M_k u_{ik} dV \quad (4.104)$$

and

$$H_{ex} = \frac{\beta_1}{2}\frac{T_c a^2}{\mu M_0}\int \frac{\partial M_l}{\partial x_i}\frac{\partial M_l}{\partial x_k} u_{ik} dV + \frac{\beta_2}{2}\frac{T_c a^2}{\mu M_0}\int \frac{\partial M_l}{\partial x_i}\frac{\partial M_l}{\partial x_i} u_{ii} dV \quad (4.105)$$

H_{ms} is the usual form of magnetoelastic energy, whose origin is complicated and mostly due to the spin orbit interaction. H_{ex} arises from the expansion of the exchange energy in the strain. [34] [86]

The authors provide a comprehensive study of magnon relaxation due to magnon

phonon. They found a much smaller relaxation time in the dipolar range than that in the exchange range. This is reasonable, because in the dipolar regime, the Cherenkov radiation of magnons to phonons is forbidden due to the fact the velocity of phonon is much large than that of magnon. The calculation gives that in the dipolar regime, the relaxation rate is about 0.13 MHz (See Fig. 7 in Ref. [73]), almost equal to the relaxation rate we obtained in our calculation due to three magnon processes! This means that in the relaxation of condensed magnons, the three magnons processes and the magnon-phonon processes are both very important.

5. CONCLUSIONS

In this work, we first review the basic quantum and classical theory of spin waves. Especially we give the quantum theory of magnons in a ferromagnetic film. Then we provide a review of the recent experimental developments in magnon BEC and of the theoretical achievements. In Section 3, we have calculated the 4-th order magnon-magnon interactions in the condensate of a film of YIG, including magnon non-conserving term responsible for the coherence of two condensates. We predict a phase transition from symmetric to nonsymmetric state that happens at a reasonable magnetic field $H = 0.2$ kOe in sufficiently thin YIG films $d = 0.1$ mm. We also predict that within the non-symmetric state there is a thickness $d*(H)$ where the modulation in the observed interference pattern should totally disappear.

In Section 4, we calculated the relaxation rate of condensed magnons in the ferromagnetic YIG film with a finite thickness. Our result shows that the three magnon processes are important in determining the relaxation rate. It is of the same order of that provided by magnon-phonon interaction.

REFERENCES

[1] J. F. Allen and A. D. Misener. Flow of liquid helium II. *Nature*, 141(3558):75, 1938.

[2] A. Amo, D. Sanvitto, F. P. Laussy, D. Ballarini, E. Del Valle, M. D. Martin, A. Lemaitre, J. Bloch, D. N. Krizhanovskii, M. S. Skolnick, and *et al.* Collective fluid dynamics of a polariton condensate in a semiconductor microcavity. *Nature*, 457(7227):291–295, 2009.

[3] Alberto Amo, Jérôme Lefrère, Simon Pigeon, Claire Adrados, Cristiano Ciuti, Iacopo Carusotto, Romuald Houdré, Elisabeth Giacobino, and Alberto Bramati. Superfluidity of polaritons in semiconductor microcavities. *Nature Physics*, 5(11):805–810, 2009.

[4] Mike H. Anderson, Jason R. Ensher, Michael R. Matthews, Carl E. Wieman, and Eric A. Cornell. Observation of bose-einstein condensation in a dilute atomic vapor. *Science*, 269(5221):198–201, 1995.

[5] R. Balili, V. Hartwell, D. Snoke, L. Pfeiffer, and K. West. Bose-einstein condensation of microcavity polaritons in a trap. *Science*, 316(5827):1007–1010, 2007.

[6] John M. Blatt, K. W. Böer, and Werner Brandt. Bose-einstein condensation of excitons. *Physical Review*, 126(5):1691, 1962.

[7] N. Bogolubov. On the theory of superfluidity. *Journal of Physics*, 11:23–29, 1966.

[8] Yuriy M. Bunkov and Grigory E. Volovik. Bose-einstein condensation of magnons in superfluid ^{3}he. *Journal of Low Temperature Physics*, 150(3):135–

144, 2008.

[9] Yuriy M. Bunkov and Grigory E. Volovik. Magnon bose–einstein condensation and spin superfluidity. *Journal of Physics: Condensed Matter*, 22(16):164210, 2010.

[10] L. V. Butov, A. L. Ivanov, A. Imamoglu, P. B. Littlewood, A. A. Shashkin, V. T. Dolgopolov, K. L. Campman, and A. C. Gossard. Stimulated scattering of indirect excitons in coupled quantum wells: Signature of a degenerate bose-gas of excitons. *Phys. Rev. Lett.*, 86(4):5608–5611, 2001.

[11] Vladimir Cherepanov, Igor Kolokolov, and Victor L'vov. The saga of yig: spectra, thermodynamics, interaction and relaxation of magnons in a complex magnet. *Physics Reports*, 229(3):81–144, 1993.

[12] A. L. Chernyshev. Field dependence of magnon decay in yttrium iron garnet thin films. *Physical Review B*, 86(6):060401, 2012.

[13] A. V. Chumak, G. A. Melkov, V. E. Demidov, O. Dzyapko, V. L. Safonov, and S. O. Demokritov. Bose-einstein condensation of magnons under incoherent pumping. *Phys. Rev. Lett.*, 102:187205, May 2009.

[14] Michele Correggi, Alessandro Giuliani, and Robert Seiringer. Validity of spin wave theory for the quantum heisenberg model. *arXiv preprint arXiv:1404.4717*, 2014.

[15] R. N. Costa Filho, M. G. Cottam, and G. A. Farias. Microscopic theory of dipole-exchange spin waves in ferromagnetic films: Linear and nonlinear processes. *Physical Review B*, 62(10):6545, 2000.

[16] R. W. Damon and J. R. Eshbach. Magnetostatic modes of a ferromagnet slab. *Journal of Physics and Chemistry of Solids*, 19(3):308–320, 1961.

[17] K. B. Davis, M.-O. Mewes, M. R. Andrews, N. J. Van Druten, D. S. Durfee, D. M. Kurn, and W. Ketterle. Bose-einstein condensation in a gas of sodium atoms. *Phys. Rev. Lett.*, 75(22):3969, 1995.

[18] V. E. Demidov, O. Dzyapko, M. Buchmeier, T. Stockhoff, G. Schmitz, G. A. Melkov, and S. O. Demokritov. Magnon kinetics and bose-einstein condensation studied in phase space. *Physical Review Letters*, 101(25):257201, 2008.

[19] V. E. Demidov, O. Dzyapko, S. O. Demokritov, G. A. Melkov, and A. N. Slavin. Thermalization of a parametrically driven magnon gas leading to bose-einstein condensation. *Phys. Rev. Lett.*, 99(3):037205, 2007.

[20] V. E. Demidov, O. Dzyapko, S. O. Demokritov, G. A. Melkov, and A. N. Slavin. Observation of spontaneous coherence in bose-einstein condensate of magnons. *Phys. Rev. Lett.*, 100(4):047205, 2008.

[21] S. O. Demokritov, V. E. Demidov, O. Dzyapko, G. A. Melkov, A. A. Serga, B. Hillebrands, and A. N. Slavin. Bose–einstein condensation of quasi-equilibrium magnons at room temperature under pumping. *Nature*, 443(7110):430–433, 2006.

[22] S. O. Demokritov, V. E. Demidov, O. Dzyapko, G. A. Melkov, and A. N. Slavin. Quantum coherence due to bose–einstein condensation of parametrically driven magnons. *New Journal of Physics*, 10(4):045029, 2008.

[23] Sergej O. Demokritov and Andrei N. Slavin. *Magnonics: From Fundamentals to Applications*. Springer, 2012.

[24] I. Dzyaloshinsky. A thermodynamic theory of weak ferromagnetism of antiferromagnetics. *Journal of Physics and Chemistry of Solids*, 4(4):241–255, 1958.

[25] O. Dzyapko, V. E. Demidov, M. Buchmeier, T. Stockhoff, G. Schmitz, G. A. Melkov, and S. O. Demokritov. Excitation of two spatially separated bose-einstein condensates of magnons. *Phys. Rev. B*, 80(6):060401, 2009.

[26] O. Dzyapko, V. E. Demidov, S. O. Demokritov, G. A. Melkov, and V. L. Safonov. Monochromatic microwave radiation from the system of strongly excited magnons. *Applied Physics Letters*, 92(16):162510, 2008.

[27] O. Dzyapko, V. E. Demidov, S. O. Demokritov, G. A. Melkov, and A. N. Slavin. Direct observation of bose–einstein condensation in a parametrically driven gas of magnons. *New Journal of Physics*, 9(3):64, 2007.

[28] O. Dzyapko, V. E. Demidov, and Sergei Olegovich Demokritov. Kinetics and bose-einstein condensation of parametrically driven magnons at room temperature. *Physics-Uspekhi*, 53(8):853–858, 2010.

[29] H. Fröhlich. Bose condensation of strongly excited longitudinal electric modes. *Physics Letters A*, 26(9):402–403, 1968.

[30] Thierry Giamarchi, Christian Rüegg, and Oleg Tchernyshyov. Bose–einstein condensation in magnetic insulators. *Nature Physics*, 4(3):198–204, 2008.

[31] Johannes Hick, Thomas Kloss, and Peter Kopietz. Thermalization of magnons in yttrium-iron garnet: Nonequilibrium functional renormalization group approach. *Physical Review B*, 86(18):184417, 2012.

[32] Johannes Hick, Francesca Sauli, Andreas Kreisel, and Peter Kopietz. Bose-einstein condensation at finite momentum and magnon condensation in thin film ferromagnets. *European Physical Journal B*, 78(4):429–437, 2010.

[33] M. J. Jones and M. G. Cottam. A study of spin–phonon interactions in ferromagnetic insulators. i. the spin wave spectrum. *Physica Status Solidi*, 66(2):651–662,

1974.

[34] M. I. Kaganov and V. M. Tsukernik. Phenomenological theory of kinetic processes in ferromagnetic dielectrics. 2. interaction of spin waves with phonons. *Soviet Physics JETP-USSR*, 9(1):151–156, 1959.

[35] Moisei I. Kaganov, N. B. Pustyl'nik, and T. I. Shalaeva. Magnons, magnetic polaritons, magnetostatic waves. *Physics-Uspekhi*, 40(2):181, 1997.

[36] Yu D. Kalafati and V. L. Safonov. Possibility of bose condensation of magnons excited by incoherent pump. *JETP Lett*, 50(3), 1989.

[37] Yu D. Kalafati and V. L. Safonov. The theory of quasi equilibrium effects in a magnon system excited with incoherent pumping. *Zhurnal Eksperimentalnoii Teoreticheskoi Fiziki*, 100(5):1511–1521, 1991.

[38] Yu D. Kalafati and V. L. Safonov. Theory of bose condensation of magnons excited by noise. *Journal of Magnetism and Magnetic Materials*, 123(1):184–186, 1993.

[39] B. A. Kalinikos. Excitation of propagating spin waves in ferromagnetic films. *Microwaves, Optics and Antennas, IEE Proceedings H*, 127(1):4, 1980.

[40] B. A. Kalinikos. Spectrum and linear excitation of spin waves in ferromagnetic films. *Russian Physics Journal*, 24(8):718–731, 1981.

[41] B. A. Kalinikos, N. G. Kovshikov, and A. N. Slavin. Observation of spin-wave solitons in ferromagnetic films. *JETP Letters*, 38(7):413–417, 1983.

[42] P. Kapitza. Viscosity of liquid helium below the l-point. *Nature*, 141(3558):74, 1938.

[43] Jacek Kasprzak, M. Richard, S. Kundermann, A. Baas, P. Jeambrun, J. M. J. Keeling, F. M. Marchetti, M. H. Szymańska, R. Andre, J. L. Staehli, et al.

Bose–einstein condensation of exciton polaritons. *Nature*, 443(7110):409–414, 2006.

[44] C. Kittel. Interaction of spin waves and ultrasonic waves in ferromagnetic crystals. *Physical Review*, 110(4):836, 1958.

[45] C. Kittel and E. Abrahams. Relaxation process in ferromagnetism. *Reviews of Modern Physics*, 25(1):233, 1953.

[46] J. Klaers, J. Schmitt, F. Vewinger, and M. Weitz. Bose-einstein condensation of photons in an optical microcavity. *Nature*, 468(7323):545–548, 2010.

[47] Thomas Kloss, Andreas Kreisel, and Peter Kopietz. Parametric pumping and kinetics of magnons in dipolar ferromagnets. *Physical Review B*, 81(10):104308, 2010.

[48] Andreas Kreisel, Francesca Sauli, Lorenz Bartosch, and Peter Kopietz. Microscopic spin-wave theory for yttrium-iron garnet films. *European Physical Journal B*, 71(1):59–68, 2009.

[49] Pavol Krivosik and Carl E. Patton. Hamiltonian formulation of nonlinear spin-wave dynamics: Theory and applications. *Phys. Rev. B*, 82(18):184428, 2010.

[50] Hidekazu Kurebayashi, Oleksandr Dzyapko, Vladislav E Demidov, Dong Fang, A. J. Ferguson, and Sergej O. Demokritov. Controlled enhancement of spin-current emission by three-magnon splitting. *Nature Materials*, 10(9):660–664, 2011.

[51] L. D. Landau and E. M. Lifshitz. *Statistical physics, vol. 5 of Course of Theoretical Physics*. Elsevier, 1980.

[52] Anthony J. Leggett. Bose-einstein condensation in the alkali gases: Some fundamental concepts. *Rev. Mod. Phys.*, 73(2):307, 2001.

[53] Fuxiang Li, Wayne M. Saslow, and Valery L. Pokrovsky. Phase diagram for magnon condensate in yttrium iron garnet film. *Scientific Reports*, 3, 2013.

[54] Fritz London. On the bose-einstein condensation. *Physical Review*, 54(11):947, 1938.

[55] Otger Jan Luiten, HGC Werij, I. D. Setija, M. W. Reynolds, T. W. Hijmans, and J. T. M. Walraven. Lyman-α spectroscopy of magnetically trapped atomic hydrogen. *Physical Review Letters*, 70(5):544, 1993.

[56] L. V. Lutsev. Dispersion relations and low relaxation of spin waves in thin magnetic films. *Physical Review B*, 85(21):214413, 2012.

[57] Otfried Madelung. *Introduction to solid-state theory*. Springer, 1996.

[58] B. A. Malomed, O. Dzyapko, V. E. Demidov, and S. O. Demokritov. Ginzburg-landau model of bose-einstein condensation of magnons. *Phys. Rev. B*, 81(2):024418, 2010.

[59] Naoto Masuhara, John M. Doyle, Jon C. Sandberg, Daniel Kleppner, Thomas J. Greytak, Harald F. Hess, and Greg P. Kochanski. Evaporative cooling of spin-polarized atomic hydrogen. *Physical Review Letters*, 61(8):935, 1988.

[60] Christoph Mathieu, Valeri T. Synogatch, and Carl E. Patton. Brillouin light scattering analysis of three-magnon splitting processes in yttrium iron garnet films. *Physical Review B*, 67(10):104402, 2003.

[61] G. A. Melkov, V. L. Safonov, A. Yu Taranenko, and S. V. Sholom. Kinetic instability and bose condensation of nonequilibrium magnons. *Journal of Magnetism and Magnetic Materials*, 132(1):180–184, 1994.

[62] Tôru Moriya. New mechanism of anisotropic superexchange interaction. *Physical Review Letters*, 4(5):228, 1960.

[63] Svâtoslav Anatol'evič Moskalenko and David W. Snoke. *Bose-Einstein condensation of excitons and biexcitons: and coherent nonlinear optics with excitons*. Cambridge University Press, 2000.

[64] T. Nikuni, M. Oshikawa, A. Oosawa, and H. Tanaka. Bose-einstein condensation of dilute magnons in tlcucl 3. *Physical Review Letters*, 84(25):5868, 2000.

[65] Wolfgang Nolting and Anupuru Ramakanth. *Quantum theory of magnetism*. Springer, 2009.

[66] P. Nowik-Boltyk, O. Dzyapko, V. E. Demidov, N. G. Berloff, and S. O. Demokritov. Spatially non-uniform ground state and quantized vortices in a two-component bose-einstein condensate of magnons. *Scientific Reports*, 2, 2012.

[67] César L Ordóñez-Romero, Boris A Kalinikos, Pavol Krivosik, Wei Tong, Pavel Kabos, and Carl E. Patton. Three-magnon splitting and confluence processes for spin-wave excitations in yttrium iron garnet films: Wave vector selective brillouin light scattering measurements and analysis. *Physical Review B*, 79(14):144428, 2009.

[68] P. Pincus, M. Sparks, and R. C. LeCraw. Ferromagnetic relaxation. ii. the role of four-magnon processes in relaxing the magnetization in ferromagnetic insulators. *Physical Review*, 124(4):1015, 1961.

[69] Erling Pytte. Spin-phonon interactions in a heisenberg ferromagnet. *Annals of Physics*, 32(3):377–403, 1965.

[70] Sergio M. Rezende. Crossover behavior in the phase transition of the bose-einstein condensation in a microwave-driven magnon gas. *Phys. Rev. B*, 80:092409, Sep 2009.

[71] Sergio M. Rezende. Theory of coherence in bose-einstein condensation phenomena in a microwave-driven interacting magnon gas. *Phys. Rev. B*, 79(17):174411, 2009.

[72] Sergio M. Rezende. Wave function of a microwave-driven bose-einstein magnon condensate. *Phys. Rev. B*, 81(2):020414, 2010.

[73] Andreas Rückriegel, Peter Kopietz, Dmytro A Bozhko, Alexander A Serga, and Burkard Hillebrands. Magnetoelastic modes and lifetime of magnons in thin yttrium iron garnet films. *Physical Review B*, 89(18):184413, 2014.

[74] C. W. Sandweg, M. B. Jungfleisch, V. I. Vasyuchka, A. A. Serga, P. Clausen, H. Schultheiss, B. Hillebrands, A. Kreisel, and P. Kopietz. Wide-range wavevector selectivity of magnon gases in brillouin light scattering spectroscopy. *Review of Scientific Instruments*, 81(7):073902, 2010.

[75] A. A. Serga, C. W. Sandweg, V. I. Vasyuchka, M. B. Jungfleisch, B. Hillebrands, A. Kreisel, P. Kopietz, and M. P. Kostylev. Brillouin light scattering spectroscopy of parametrically excited dipole-exchange magnons. *Physical Review B*, 86(13):134403, 2012.

[76] Alexander A. Serga, Vasil S. Tiberkevich, Christian W. Sandweg, Vitaliy I. Vasyuchka, Dmytro A. Bozhko, Andrii V. Chumak, Timo Neumann, Björn Obry, Gennadii A. Melkov, Andrei N. Slavin, et al. Bose–einstein condensation in an ultra-hot gas of pumped magnons. *Nature Communications*, 5:3452, 2014.

[77] K. P. Sinha and U. N. Upadhyaya. Phonon-magnon interaction in magnetic crystals. *Physical Review*, 127(2):432, 1962.

[78] A. N. Slavin and I. V. Rojdestvenski. bright and dark spin wave envelope solitons in magnetic films. *Magnetics, IEEE Transactions On*, 30(1):37–45, 1994.

[79] Andrei Slavin and Vasil Tiberkevich. Excitation of spin waves by spin-polarized current in magnetic nano-structures. *Magnetics, IEEE Transactions On*, 44(7):1916–1927, 2008.

[80] David Snoke. Coherent questions. *Nature*, 443:403, 2006.

[81] M. Sparks. Theory of three-magnon ferromagnetic relaxation frequency for low temperatures and small wave vectors. *Physical Review*, 160(2):364, 1967.

[82] M. Sparks, R. Loudon, and C. Kittel. Ferromagnetic relaxation. i. theory of the relaxation of the uniform precession and the degenerate spectrum in insulators at low temperatures. *Physical Review*, 122(3):791, 1961.

[83] H. Suhl. The theory of ferromagnetic resonance at high signal powers. *Journal of Physics and Chemistry of Solids*, 1(4):209–227, 1957.

[84] Roberto E. Troncoso and Álvaro S. Núñez. Dynamics and spontaneous coherence of magnons in ferromagnetic thin films. *Journal of Physics: Condensed Matter*, 24(3):036006, 2012.

[85] I. S. Tupitsyn, P. C. E. Stamp, and A. L. Burin. Stability of bose-einstein condensates of hot magnons in yttrium iron garnet films. *Phys. Rev. Lett.*, 100(25):257202, 2008.

[86] V. I. Vasyuchka, A. A. Serga, C. W. Sandweg, D. V. Slobodianiuk, G. A. Melkov, and B. Hillebrands. Explosive electromagnetic radiation by the relaxation of a multimode magnon system. *Phys. Rev. Lett.*, 111:187206, Nov 2013.

[87] G. E. Volovik. Twenty years of magnon bose condensation and spin current superfluidity in ^{3}he-b. *Journal of Low Temperature Physics*, 153:266–284, 2008.

[88] Robert M. White. *Quantum theory of magnetism: magnetic properties of materials*, volume 32. Springer, 2007.

[89] Peng Yan and Gerrit E. W. Bauer. Magnonic domain wall heat conductance in ferromagnetic wires. *Physical Review Letters*, 109(8):087202, 2012.

[90] Vivien Zapf, Marcelo Jaime, and C. D. Batista. Bose-einstein condensation in quantum magnets. *Reviews of Modern Physics*, 86(2):563, 2014.